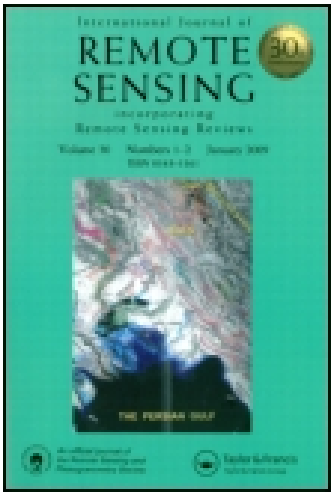

International Journal of Remote Sensing
Publication details, including instructions for authors and subscription information:
http://www.tandfonline.com/loi/tres20

A Landsat-based study of black rock coatings proximal to base metal smelters, Sudbury, Ontario, Canada

Kelly J. Malcolm[a], David W. Leverington[b] & Michael Schindler[a]
[a] Department of Earth Sciences, Laurentian University, Sudbury, ON, Canada P3E 2C6
[b] Department of Geosciences, Texas Tech University, Lubbock, TX 79409, USA
Published online: 28 Jul 2015.

International Journal of Remote Sensing, 2015
Vol. 36, No. 15, 3932–3960, http://dx.doi.org/10.1080/01431161.2015.1054963

A Landsat-based study of black rock coatings proximal to base metal smelters, Sudbury, Ontario, Canada

Kelly J. Malcolm[a], David W. Leverington[b]*, and Michael Schindler[a]

[a]*Department of Earth Sciences, Laurentian University, Sudbury, ON, Canada P3E 2C6;*
[b]*Department of Geosciences, Texas Tech University, Lubbock, TX 79409, USA*

(*Received 6 January 2015; accepted 8 April 2015*)

Past emission of metal-bearing particulate matter, sulphur dioxide (SO_2), and sulphuric acid by base metal smelters in the Sudbury region led to widespread loss of vegetation, contamination of soils, and formation of black coatings on rock surfaces. These black coatings formed through the incorporation of smelter-borne particulate matter into the partly dissolved uppermost layers of siliceous minerals on exposed rock, and are characterized by high heavy-metal content. This study involved assessment of the reflectance properties of black coatings in the Sudbury region, and determination of the geographic distribution of coatings through supervised classification of reflectance data derived from a Landsat Enhanced Thematic Mapper Plus (ETM+) image. Classifications involved the use of the Spectral Angle Mapper (SAM), Maximum Likelihood, and Feedforward Backpropagation Neural Network algorithms. The reflectance spectra of black coatings in the Sudbury region are relatively flat and featureless, and are characterized by reflectance values less than ~13% across the visible, near-infrared, and short-wave infrared. Spectral properties are similar to those of magnetite, a spinel-group mineral known to be present in Sudbury coatings. The presence of carbon-rich soot particles may be an important influence on the reflectance properties of coatings. SAM classification results are characterized by the widespread mislabelling of uncoated urban and open-pit sites as mantled by black coatings, and neural network results problematically mislabel some uncoated wetland sites as coated. Results generated by the Maximum Likelihood algorithm most usefully depict the distribution of exposed black coatings in the Sudbury region. The mapping of black coatings using remote-sensing methods can provide useful information on the spatial character of environmental degradation in the vicinity of smelters, and should be helpful in the monitoring of environmental recovery where emissions have been reduced or eliminated.

1. Introduction

Base metal smelters can act as point sources of heavy-metal and toxic-element pollution (Davies 1983; Rieuwerts and Farago 1996; Schindler et al. 2012; Mantha, Schindler, and Kyser 2012; Mantha et al. 2012). Emission of sulphur dioxide (SO_2) and sulphates from smelter stacks can create highly acidic rain that can dissolve the uppermost layer of siliceous minerals on exposed rock surfaces near smelter facilities. Following the dissolution of the siliceous minerals, a silica-gel-type material can form and trap detrital material and smelter-borne atmospheric particulate matter (Schindler et al. 2009; Mantha, Schindler, and Kyser 2012; Mantha et al. 2012). Upon solidification of this gel, a black coating is formed. These rock coatings contain anomalously high heavy-metal contents,

*Corresponding author. Email: david.leverington@ttu.edu

which are slowly leached into surrounding soils and hydrological systems (Mantha, Schindler, and Kyser 2012).

The Sudbury region of Canada hosts one of the largest nickel–copper–platinum-group-elements (Ni-Cu-PGE) deposits in the world (Keays and Lightfoot 2004; Dill 2010). Sudbury initially emerged as an important mining centre in the 1880s, and local roasting and smelting operations began at this time. Major smelting operations commenced at the Copper Cliff site by 1888, at the Coniston site by 1913, and at the Falconbridge site by 1930 (Rousell, Meyer, and Prevec 2002; Saarinen and Tanos 2002) (Figure 1). Emission of metal-bearing particulate matter and high levels of sulphates and SO_2 by smelters, combined with extensive logging activities, gradually resulted in considerable loss of vegetation in surrounding areas and led to widespread contamination of soils and formation of black coatings on exposed rock surfaces

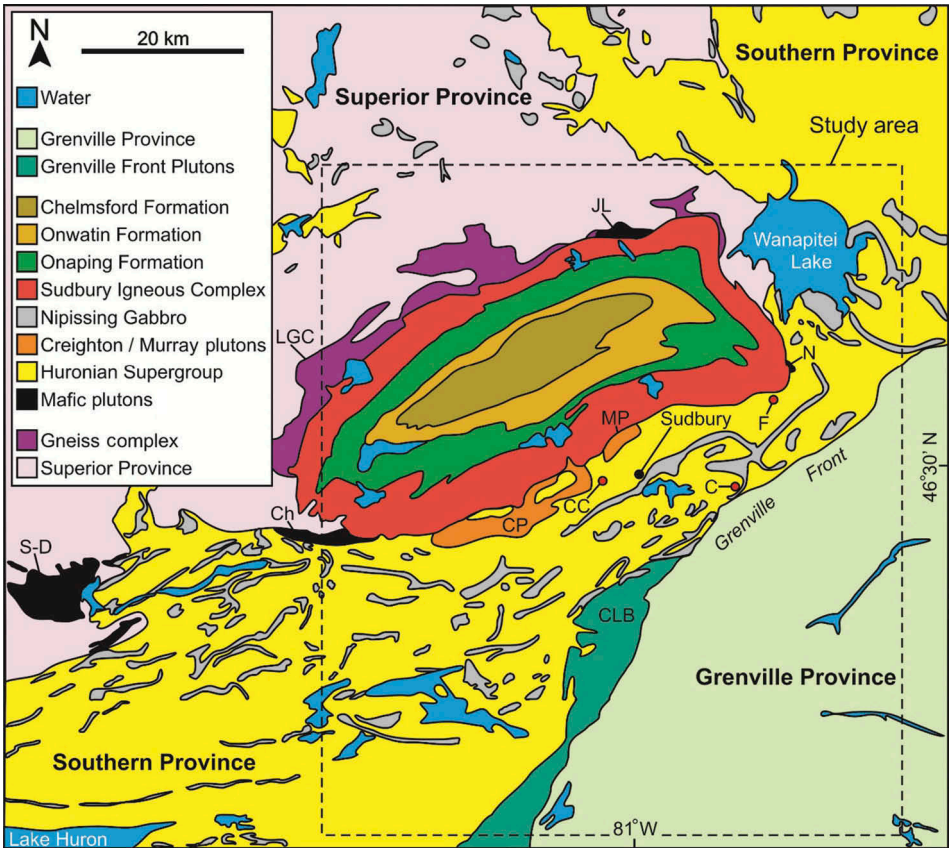

Figure 1. Simplified geological map of the Sudbury region (modified after Rousell, Meyer, and Prevec 2002; see also, for example, Card 1978b; Dressler 1984). Labelled intrusions: LGC, Levack gneiss complex; N, Norduna pluton; Ch, Chicago pluton; JL, Joe Lake pluton; S-D, Shakespeare-Dunlop pluton; CP, Creighton pluton; MP, Murray pluton; CLB, Chief Lake Batholith. Bedrock in the study area has largely been subjected to greenschist and higher grades of metamorphism. Three major smelter sites are identified by red circles: F, Falconbridge; C, Coniston; CC, Copper Cliff. The urban centre of Sudbury is identified by a black circle located near the centre of the study area.

(Winterhalder 2002; Meadows and Watmough 2012; Mantha, Schindler, and Kyser 2012). Major improvements in air quality in the 1970s and 1980s, in conjunction with land reclamation activities, led to a reversal of the earlier effects of smelting in the Sudbury region (Heale 1995; Keller, Heneberry, and Gunn 1999; Narendrula, Nkongolo, and Beckett 2012). Although this reversal continues today, it is slowed by several factors including the persistence of high levels of contaminants in near-surface materials (Winterhalder 2002; Lanteigne et al. 2012; Tanentzap and Ryser 2015).

Multispectral images have previously been used to identify the spatial distribution of general surface classes in the Sudbury region, including areas of low biomass and associated exposures of rock and sediment (e.g. Pitblado and Gallie 1995; Singhroy and Kuhn 1996; Champagne et al. 2004; Davidson and Gunn 2012), and similar work has been conducted for areas near other major smelting centres (e.g. Coulson and Bridges 1984; Mikkola 1996; Tømmervik, Johansen, and Pedersen 1995; Tømmervik, Høgda, and Solheim 2003; Toutoubalina and Rees 1999; Zubareva et al. 2003). As at other mining sites worldwide (e.g. Richter, Staenz, and Kaufmann 2008; Riaza and Müller 2010), remote-sensing techniques have been used in the Sudbury area to determine the chemistry and mineralogy of mine tailings (e.g. Shang et al. 2002, 2009). Remote-sensing techniques have also been used to better understand the environmental effects of smelter emissions in the Sudbury region. For example, Barnett and Bajc (2002) used a false-colour composite of Landsat Thematic Mapper data to highlight areas affected by human activities in the region, though this composite image does not distinguish between sites affected by smelting activities and those affected by other types of human activity such as agriculture and the exploitation of aggregate deposits. Aerial and satellite images have been successfully used to better characterize vegetation damage near Sudbury smelters and to monitor vegetation recovery (e.g. Pitblado and Amiro 1982; Mussakowski 1983; Allum and Dreisinger 1987, McCall, Gunn, and Struik 1995; Champagne et al. 2004; Abuelgasim et al. 2005; Lévesque and Staenz 2008), and related techniques have been used to monitor changes in vegetation distribution near smelters worldwide (e.g. Tømmervik, Johansen, and Pedersen 1995; Tømmervik, Høgda, and Solheim 2003, Mikkola 1996; Hagner and Rigina 1998; Rigina et al. 1999; Toutoubalina and Rees 1999; Rigina 2003). Natural environments of relevance to the formation of black rock coatings include volcanic and hydrothermal sites where acid-sulphate weathering has occurred (e.g. Schiffman et al. 2006), and remote-sensing techniques have previously been applied to the study of such environments on both Earth and Mars (e.g. Vaughan, Calvin, and Taranik 2003; Le Deit et al. 2008; Chemtob et al. 2010; Seelos et al. 2010; Marcucci et al. 2013).

This study involved the characterization of the reflectance properties of black coatings in the Sudbury region, and the use of remote-sensing methods to determine the geographic distribution of exposed coatings proximal to Sudbury base metal smelters. Supervised classification of a reflectance database generated from a Landsat Enhanced Thematic Mapper Plus (ETM+) image was conducted using (1) the Spectral Angle Mapper (SAM) algorithm, on the basis of a representative lab-measured reflectance spectrum of coated bedrock; and (2) the Maximum Likelihood and Feedforward Backpropagation Neural Network classifiers, using training sites for a set of surface-cover classes that included a coated bedrock class. In order to determine the validity of the coating databases for Sudbury, and to better understand the potential applicability of utilized techniques in the mapping of black coatings in other sites where environmental degradation has occurred

and may be ongoing, algorithm outputs were qualitatively and quantitatively compared with Sudbury ground-truth information.

2. Surface materials of the Sudbury study area

The Sudbury study area is underlain by bedrock of the Superior, Southern, and Grenville provinces (Rousell, Meyer, and Prevec 2002) (Figure 1). Late Archean rocks of the Superior Province are exposed in the northwestern part of the study area, and consist largely of metavolcanic and metasedimentary rocks, as well as granitic intrusions (Sims et al. 1980; Dressler 1984). Units of the Superior Province are generally metamorphosed to greenschist and amphibolite facies, but the Levack gneiss complex is locally metamorphosed to granulite facies (Meyn 1970; Jackson and Fyon 1991; Rousell, Meyer, and Prevec 2002). Further to the south, the study area is underlain by Early Proterozoic rocks of the Southern Province, which consist largely of volcanic, impact, and sedimentary units subjected to extensive regional metamorphism (mainly lower to upper greenschist facies, but locally to amphibolite facies) (Card 1978a). These units unconformably overlie the southern limits of the Superior Province (Sims et al. 1980). The Grenville Province is exposed in the southeastern part of the study area and consists largely of gneiss, schist, metagabbro, and mylonite (Card 1978b; Dressler 1984; Rousell, Meyer, and Prevec 2002). Large felsic plutons, such as the Chief Lake Batholith, are located along parts of the boundary zone between the Southern Province and the Grenville Province (Davidson 2001). Grenville materials are characterized by metamorphic grades as high as upper amphibolite facies (Easton 1991). Grenville materials were thrust northwestward onto the Southern Province during the ~1 Ga Grenville orogeny (Corfu and Easton 2001).

The study area is mostly underlain by materials of the Southern Province, and several key units of this province are therefore separately identified in Figure 1. Mafic intrusions, including the Joe Lake, Norduna, and Chicago plutons, are in places associated with ore-grade Ni-Cu-PGE mineralization (Rousell, Meyer, and Prevec 2002). The Huronian Supergroup is largely characterized by volcanic lithologies near its base and sedimentary units at higher levels (Nesbitt and Young 1982; Dressler 1984). Moving upward through the Huronian sequence, the Elliot Lake Group includes volcanics of the Elsie Mountain, Stobie, and Copper Cliff formations, and wacke and arkose units of the McKim Formation; the Hough Lake Group is dominated by wacke and arkose units of the Ramsay Lake, Pecors, and Mississagi formations; and the Quirke Lake and Cobalt groups similarly consist largely of wacke and arkose lithologies (Dressler 1984). In the northwestern part of the study region, Huronian outliers locally rest on materials of the Superior Province. Tholeitic magmas extensively intruded the Huronian Supergroup ~2.2 Ga before present (Corfu and Andrews 1986), forming the Nipissing Gabbro (Rousell, Meyer, and Prevec 2002).

Much of the northern half of the study area is underlain by two additional units of the Southern Province: the Whitewater Group and Sudbury Igneous Complex (Figure 1). Remnants of the Whitewater Group are today found only within the Sudbury Basin, a major geological structure that is outlined by the Sudbury Igneous Complex (Riller 2005). The Whitewater Group consists of breccia and igneous-textured rocks of the Onaping Formation, carbonates of the relatively thin Vermilion Formation, carbonates and fine clastics of the Onwatin Formation, and greywacke of the Chelmsford Formation (Rousell, Meyer, and Prevec 2002). The Sudbury Igneous Complex consists of a norite sublayer that hosts world-class Ni-Cu-PGE mineralization (Keays and

Lightfoot 2004; Dill 2010), and a 'Main Mass' that consists of norite, quartz gabbro, and granophyre (Rousell, Meyer, and Prevec 2002). The Sudbury basin, the Sudbury Igneous Complex, and the Onaping Formation are believed to be the products of a 1.85 Ga impact event (e.g. Grieve et al. 2010).

Topographic relief in the study area is less than 250 m. Preserved glacial landforms in the Sudbury region include moraines, eskers, and glaciolacustrine features such as those of glacial Lake Algonquin (Barnett and Bajc 2002; Heath and Karrow 2007). Although sediment thicknesses in the Sudbury region can exceed 50 m along some river valleys and at other topographic lows, unconsolidated sedimentary deposits are generally thin (less than 1 m) and discontinuous, and bedrock exposure is good (Barnett and Bajc 2002). The natural vegetation in the region is mixed deciduous boreal forest, consisting of varieties such as red and white pine (*Pinus resinosa* and *Pinus strobus*), jack pine (*Pinus banksiana*), black and white spruce (*Picea mariana* and *Picea glauca*), balsam fir (*Abies balsamea*), sugar maple (*Acer saccharum*), yellow and white birch (*Betula alleghaniensis* and *Betula papyrifera*), and white cedar (*Thuja occidentalis*) (Winterhalder 1995). Local smelting and logging activities converted vegetation in the immediate vicinity of Sudbury from forest to woodland, savannah, and treeless barrens (Hutchinson and Whitby 1977). Dramatic improvements in air quality in the 1970s resulted from construction of the 380 m "Inco Superstack" at the Copper Cliff smelter and from closure of the Coniston smelter, but local expansion of plant colonization (McCall, Gunn, and Struik 1995; Keller, Heneberry, and Gunn 1999) continues to be suppressed where soil erosion was extensive and where high levels of metal contaminants persist in near-surface materials (Winterhalder 2002; Meadows and Watmough 2012; Nkongolo et al. 2013).

3. Formation of black coatings near base metal smelters

Rock coatings can be an excellent indicator of atmospheric and surficial conditions at the time of formation (Buzek and Šrámek 1985; Loendorf 1991; Liu and Broecker 2007; Dorn 2009; Sánchez et al. 2009; Mantha et al. 2012; Krinsley et al. 2013). Rock coatings can form due to biological (Garcia-Vallès et al. 1997; Tani et al. 2003), physical (Dixon et al. 2002, Durocher and Schindler 2011), and chemical processes (Schindler et al. 2012; Sanjurjo-Sánchez, Romaní, and Alves 2012). Three essential processes are required for the development of rock coatings: erosion of an exposed rock surface; transportation of coating components to the host rock surface; and biogeochemical barriers that prevent post-deposition movement of coating components (Dorn 1998).

Base metal smelters are known to be sources of metal contamination in adjacent surficial materials (Davies 1983; Rieuwerts and Farago 1996; Schindler et al. 2012; Mantha, Schindler, and Kyser 2012; Mantha et al. 2012). Metal contamination can be found in soils (e.g. Haneberg, Austin, and Brandvold 1993; Barcan and Kovnatsky 1998; Lanteigne et al. 2012; Lanteigne, Schindler, and McDonald 2014), animal tissues (e.g. Bagatto and Alikhan 1987; Bagatto and Shorthouse 1996), vegetation (e.g. Cui et al. 2004; Abercrombie et al. 2011), bodies of water (e.g. Alpay et al. 2006; Mayer et al. 2007), and rock coatings (e.g. Schindler et al. 2012; Mantha, Schindler, and Kyser 2012; Mantha et al. 2012). The degree of contamination is largely controlled by the type of smelter ore, the amount of emitted particulate matter, the height of smelter stacks, and the distance from the smelter facility (e.g. Svendsen, Steinnes, and Blom 2007). Airborne contamination in mineral-processing smelter facilities commonly occurs via the emission of aerosols and particulate matter from smelter stacks, refineries, tailings, and ore piles, as

well as from historical roast yards (McMartin et al. 2002). The emitted pollutants may include sulphates, SO_2, CO_2, perfluorocarbons, and elements such as Fe, Ni, Cu, Pb, Sn, Al, As, and Hg, depending on the type of ore that is being processed and the pollution controls that are in place (Mantha, Schindler, and Kyser 2012; Mantha 2012).

Smelter-related black rock coatings form on a wide spectrum of weathered igneous and metamorphic rock-types, ranging from highly felsic rhyolites to ultramafic pyroxenites and their metamorphosed equivalents. They form due to the combination of several processes. Extremely high levels of sulphates and SO_2, emitted from the smelter stacks interact with atmospheric components such as H_2O, OH, ozone and particulate matter, forming H_2SO_3/H_2SO_4-bearing aerosols. Wet deposition of these aerosols in the form of highly acidic rain results in the loss of vegetation and increased weathering of the underlying siliceous rock. A silica-gel type coating forms due to the incongruent dissolution of the silicate minerals under acidic condition (Hellmann et al. 2003), which over time hardens into amorphous and crystalline polymorphs of SiO_2. During its formation and hardening processes, the silica gel encapsulates detrital material from surrounding soils as well as smelter-borne particulate matter (Mantha, Schindler, and Kyser 2012). The latter particulate matter form as a result of the partial reaction, melting, and rapid cooling of flux and slag dust during the smelting process (Lanteigne et al. 2012). They often occur as spherical nanometre-to-micrometre-size Fe-oxide-silicates and Fe-oxides, and nanometre-size C-rich spheres (Mantha 2012); oxides such as magnetite are common products of combustion processes (e.g. Zajzon et al. 2013). The black colour that is associated with coatings, which is atypical of silica-rich rock coatings, is likely due to a high density of metal(loid)-rich nanometre-to-micrometre-sized particulates and precipitates within the silica matrix (Mantha, Schindler, and Kyser 2012; Mantha et al. 2012, Schindler et al. 2012).

4. Mineralogy of black coatings in the Sudbury study area

Landscapes located within tens of kilometres of Sudbury smelters were subjected to substantial loss of vegetation over time, particularly where concentrations of sulphates and SO_2 were greatest and where logging activities were concentrated (Winterhalder 1995; Barnett and Bajc 2002) (Figure 2). Bedrock surfaces exposed near smelters gradually became covered by black coatings (Figures 3 and 4). Coatings in the Sudbury region range in thickness from <5 to >100 μm, with a maximum observed thickness of 200 μm at locations closest to the sites of past roasting and smelting activities. Silicate minerals in underlying rock are variably weathered, and coatings and related detritus are occasionally seen in cracks between weathered minerals. The silica matrix is composed of an opal-like amorphous SiO_2 and occasional SiO_2 polymorphs (cristobalite and trydimite) (Schindler et al. 2009). These phases form from non-stoichiometric dissolution of silicate minerals under acidic conditions and subsequent hardening of the silica gel-type material. Detrital particles originate from underlying rock or adjacent soil, and are composed of a varying mixture of feldspars, amphiboles, quartz, phyllosilicates, and hematite. Smelter-derived nanometre-to-micrometre-size spherical particulates are the most abundant particles (~10–30% modal abundance) in the coatings (Figure 5; Schindler et al. 2012). They form during smelting and ore-refining processes, are transported via atmospheric processes, and are subsequently deposited in the silica gel-type matrix. The particulates mainly consist of minerals of the spinel group ($X^{2+}Y^{3+}{}_2O_4$) including magnetite (Fe_3O_4), cuprospinel ($CuFe_2O_4$), and trevorite ($NiFe_2O_4$). High-temperature silicates such as minerals of the olivine group are also present. Nanometre-sized spherical soot

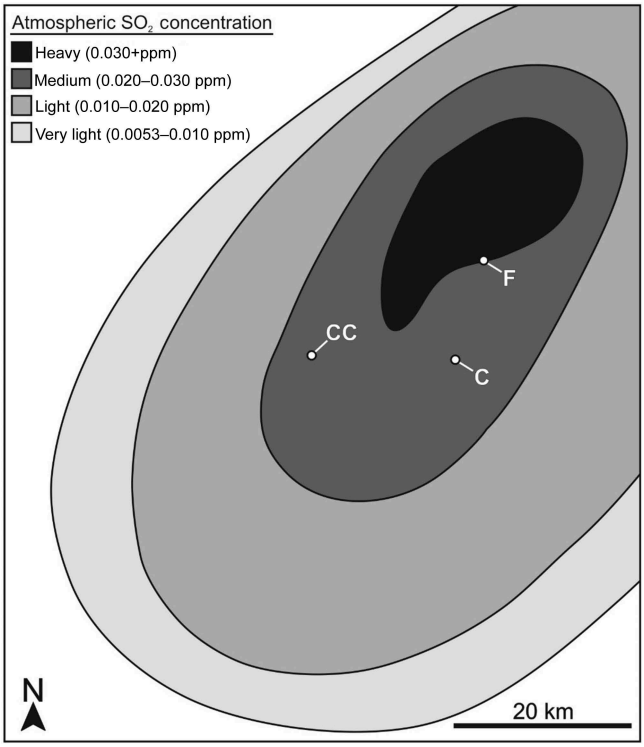

Figure 2. Mean atmospheric concentrations of SO_2 in the Sudbury study area between 1953 and 1967 (modified after Dreisinger and McGovern 1969; Winterhalder 2002). Concentrations are given in parts per million. High atmospheric concentrations of sulphates and SO_2 in the nineteenth and twentieth centuries gradually led to formation of black coatings on rock surfaces exposed near smelter sites. Labelled smelter sites: F, Falconbridge; C, Coniston; CC, Copper Cliff. See Figure 1 for study area location.

Figure 3. Coated (white arrow at top) and uncoated (black arrow at right) surfaces of an outcrop of the Stobie Formation (basalt) in the Sudbury region. Pen at centre for scale.

Figure 4. Examples of bedrock outcrops in the Sudbury region that are partly or completely mantled by black coatings: (*a*) McKim Formation; (*b*) Copper Cliff Formation; (*c*) Mississagi Formation; (*d*) Grenville gneiss; (*e*) Nipissing Gabbro; (*f*) Stobie Formation; (*g*) Elsie Mountain Formation; (*h*) Chief Lake quartz monzonite.

particulates that lack any structural long-range order are typically present in coatings, and are carbon-rich products of incomplete combustion of fossil fuels.

Metal-sulphate-rich layers in the Sudbury region are often present at either the interface between the atmosphere and the coating (Figure 5) or the interface between the

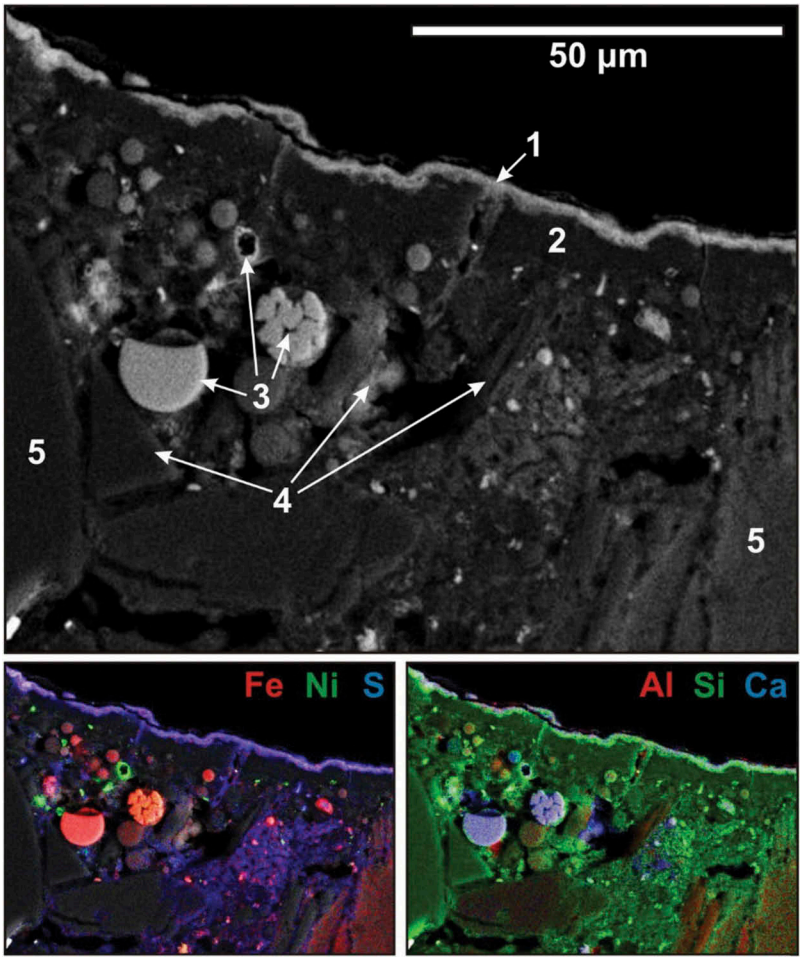

Figure 5. SEM image of a black coating from the Sudbury study area: 1, metal-rich sulphate layer at the interface between the coating and the atmosphere; 2, amorphous Si-gel matrix; 3, smelter-derived spherical particulates; 4, detrital sub-angular particulates; 5, underlying silicate minerals of the Copper Cliff rhyolite. Rasterized energy-dispersive X-ray spectroscopy (EDS) maps are given at bottom for selected elements.

underlying rock and the coating. They are composed of nanometre-scale crystals of a wide variety of Fe-rich sulphates containing significant concentrations of other metals and metalloids such as Cu, Pb, As, and Se (Mantha, Schindler, and Kyser 2012). The chemical constituents of these sulphates were most likely derived from dissolution of underlying siliceous rocks, particulate matter, and metal-sulphate-bearing aerosols under acidic conditions. The close association of these sulphates with phyllosilicates indicates that confined pore spaces in the silica matrix inhibit equilibration between the former (stable under acidic conditions) and the latter minerals (stable under near neutral pH conditions). Surface-sensitive analytical studies indicate further that metal-sulphate-rich layers along the coating–atmosphere interface are depleted in metals on the nanometre scale (Mantha, Schindler, and Kyser 2012). This observation suggests that the thickness of the coatings decreases annually by several nanometres through chemical weathering.

5. Reflectance properties of coated bedrock

The reflectance properties of rocks and sediments in the visible, near-infrared, and short-wave infrared ranges are largely determined by the materials that form the upper several hundred micrometres of their surfaces. As a result, the reflectance spectra of rocks and soils can be masked by surface materials such as alteration rinds, desert varnish, or lichen cover (e.g. Farr and Adams 1984; Rivard et al. 1992; Zhang, Rivard, and Sanchez-Azofeifa 2004; Schiffman et al. 2006; McSween, Taylor, and Wyatt 2009, Rogge et al. 2014). In this study, the reflectance characteristics of representative rock samples were investigated for the 400–2500 nm range using an Analytical Spectral Devices FieldSpec3 spectroradiometer equipped with a contact probe and integrated light source. This system has a spectral resolution of ~3–12 nm, depending on the wavelength. Samples of coated and uncoated bedrock were collected from a wide variety of geological units in the study area, and the reflectance characteristics of these samples were measured in a controlled lab setting using the contact probe. The system was calibrated on the basis of standard techniques using a white Lambertian reference panel. The spectroradiometer measures relative reflectance (the 'reflectance factor'), which is the ratio of electromagnetic radiation reflected off a sample to that reflected off the reference panel under the same conditions (e.g. Schaepman-Strub et al. 2006). The reflectance factor approximates reflectance and is referred to as such in the discussion below.

In the Sudbury study area, a wide variety of sedimentary and igneous lithologies exists, most of which have been metamorphosed to greenschist or higher facies (Rousell, Meyer, and Prevec 2002). However, the otherwise diverse range expected of the reflectance spectra of these materials can be effectively masked by the presence of black coatings. Regardless of the chemical and mineralogical nature of underlying geological materials, materials covered by black coatings in the Sudbury study area typically have relatively flat and featureless reflectance spectra, and reflectance values of less than ~13% over the 400–2500 nm range (Figures 6 and 7). Although the spectra of black coatings are distinct from those of most local lithologies, they can be somewhat similar in form and overall albedo to those of uncoated materials of units including the Copper Cliff and McKim formations (Figure 6).

Weak absorption features variously exist in some coating spectra near 950–1000, 1400, 1915, 2200, 2210, 2260, 2310, 2350, and 2385 nm (Figure 6). The features near 1400 and 1915 nm are consistent with the presence of water, and wide and shallow absorption features centred in some spectra near 950–1000 nm are consistent with the presence of iron-bearing minerals (e.g. Cloutis 2011). Absorption features near 2350 nm suggest the possible presence of carbonates (e.g. Gaffey 1985), but precipitation or preservation of carbonates at the low pH conditions involved in the formation of these coatings is unlikely. Instead, along with features such as those near 2200 and 2210 nm, the 2350 nm features are more likely to be related to the presence of hydroxide-bearing minerals such as clays and Fe-hydroxides (e.g. Sultan et al. 1987; van der Meer 2004), which are confirmed components of Sudbury black coatings. Other relevant hydroxide-bearing minerals include K- and Fe-rich sulphates (possibly including jarosite, a mineral that has not yet been confirmed in Sudbury coatings), which are typically present as thin films (Figure 5); absorption features such as those near 950–1000, 2210, and 2260 nm correlate with several of the expected features of some forms of jarosite (e.g. Shang et al. 2002, 2009; Bishop and Murad 2005; Cloutis et al. 2006). Overall, the Sudbury black coatings have reflectance properties similar to those of magnetite (Figure 7), a confirmed

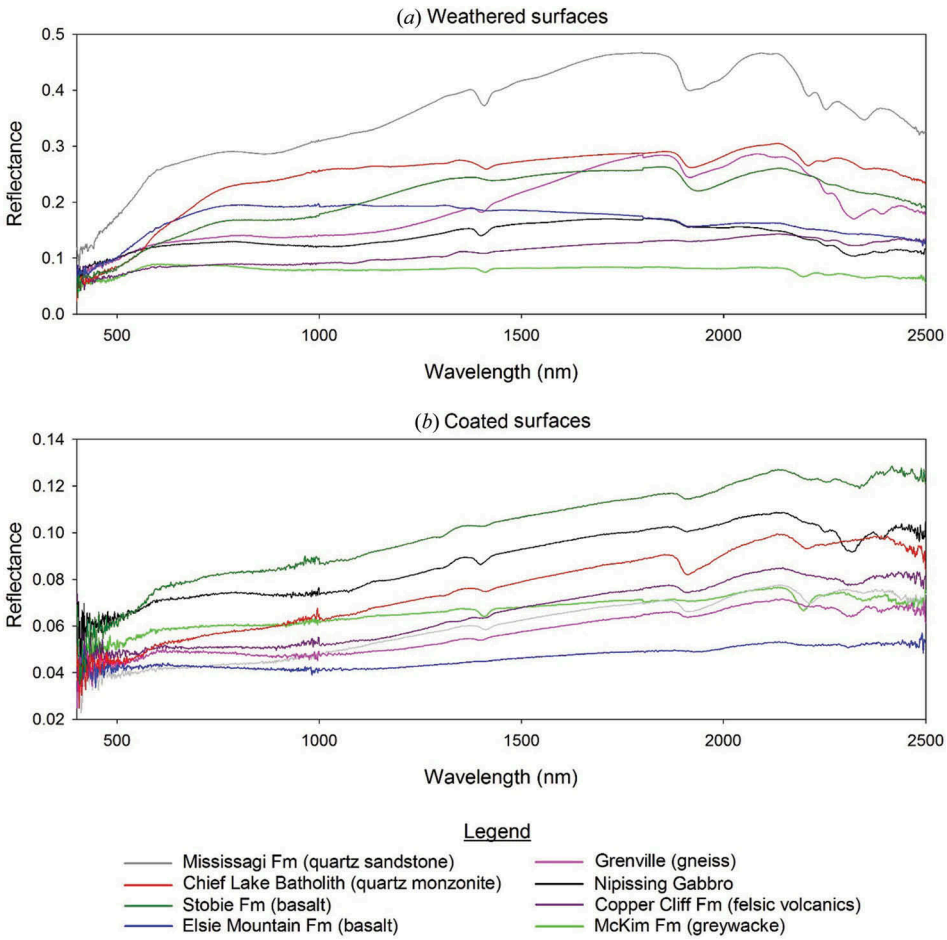

Figure 6. Examples of typical reflectance spectra for weathered rock surfaces of the Sudbury region (*a*) and for equivalent surfaces covered by black coatings (*b*). Black coatings have relatively low reflectance (less than ~13%) across the 400–2500 nm range, and are effective in blocking the spectral expression of underlying minerals.

spinel-group component of these coatings. Chromium has been detected in the Fe-rich oxides of coatings, but the presence of the spinel-group mineral chromite has not been confirmed and the spectra of coatings do not suggest the substantial presence of this mineral. Although coating spectra do not have properties expected of opaline silica, the spectra of carbon-bearing materials are typically characterized by relatively low albedo and a paucity of prominent absorption features (e.g. Cloutis, Gaffey, and Moslow 1994) and the presence of carbon-rich soot particles embedded in the opal-like silica of coatings may correspondingly help to contribute such properties to the spectra of coatings (Figure 7).

The absence of prominent peaks and troughs in the spectra of black coatings has the potential to make confident discrimination of these materials challenging. Also, similarities between the spectral characteristics of black coatings and uncoated materials of units including the Copper Cliff and McKim formations suggest the potential for confusion

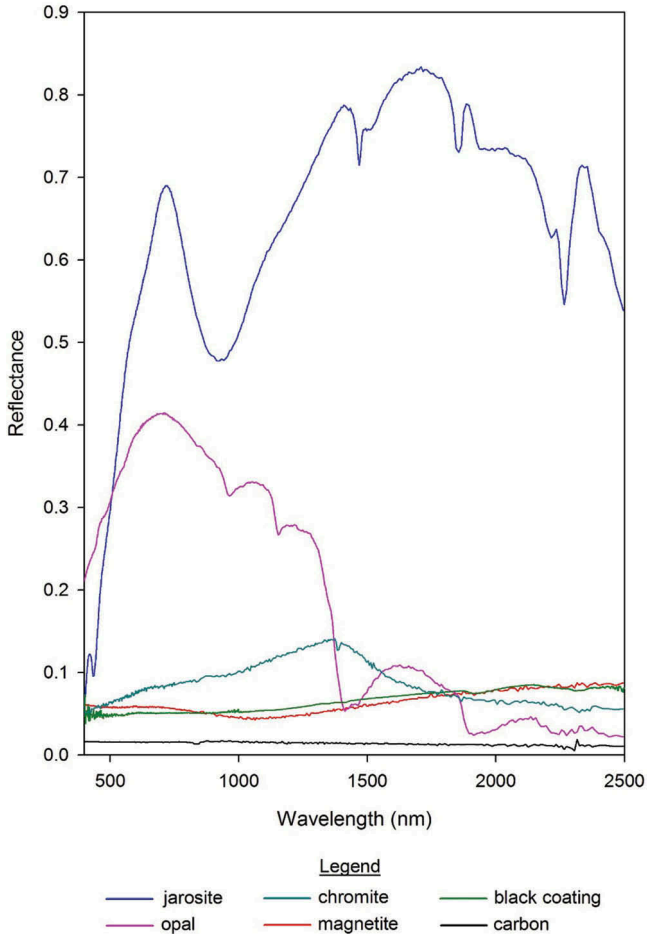

Figure 7. Reflectance spectra for a black coating sample and for several materials relevant to coatings. Black coating reflectance data were determined from a sample of the Copper Cliff Formation (Figure 6). Other reflectance data courtesy of the Spectral Library of the United States Geological Survey (USGS) Spectroscopy Lab (Clark et al. 2007): jarosite sample JR2501, opal sample WS132, chromite sample HS281, magnetite sample HS195, carbon sample JDS68.

between these classes. However, good exposures of such units are mostly found within tens of kilometres of local smelters and are typically covered by black coatings, reducing the likelihood of errors of commission (i.e. incorrect identification of coated materials at uncoated sites). Overall, the relative consistency of the spectral properties of black coatings in the Sudbury area, combined with the partial or absent vegetative cover that is typical of extensively coated bedrock surfaces, makes the discrimination of black coatings in remote-sensing images feasible.

6. Remote-sensing data and classification methodology

This study involved the use of a surface reflectance database produced by the Global Land Cover Facility (GLCF, University of Maryland) from a Landsat ETM+

multispectral image collected by Landsat-7 on 27 August 2000 (scene ID 238–469). This orthorectified database falls within the 019/028 coordinate of the Worldwide Reference System, and has a pixel size of 30 m × 30 m. The GLCF generates databases of surface reflectance from ETM+ images using a standardized methodology that is based in part on the 6S radiative transfer model (Masek et al. 2006; Feng et al. 2013). This study focused on the use of reflectance data derived from band 1 (450–515 nm), band 2 (525–605 nm), band 3 (630–690 nm), band 4 (750–900 nm), band 5 (1550–1750 nm), and band 7 (2090–2350 nm) (Figure 8). These bands cover several key parts of the visible, near-infrared, and short-wave infrared ranges that are useful in the discrimination of geological and other surface-cover classes (e.g. Flynn, Harris, and Wright 2001; Leverington 2010; Xiong et al. 2011; Behnia et al. 2012; Cracknell and Reading 2014; Harris et al. 2014).

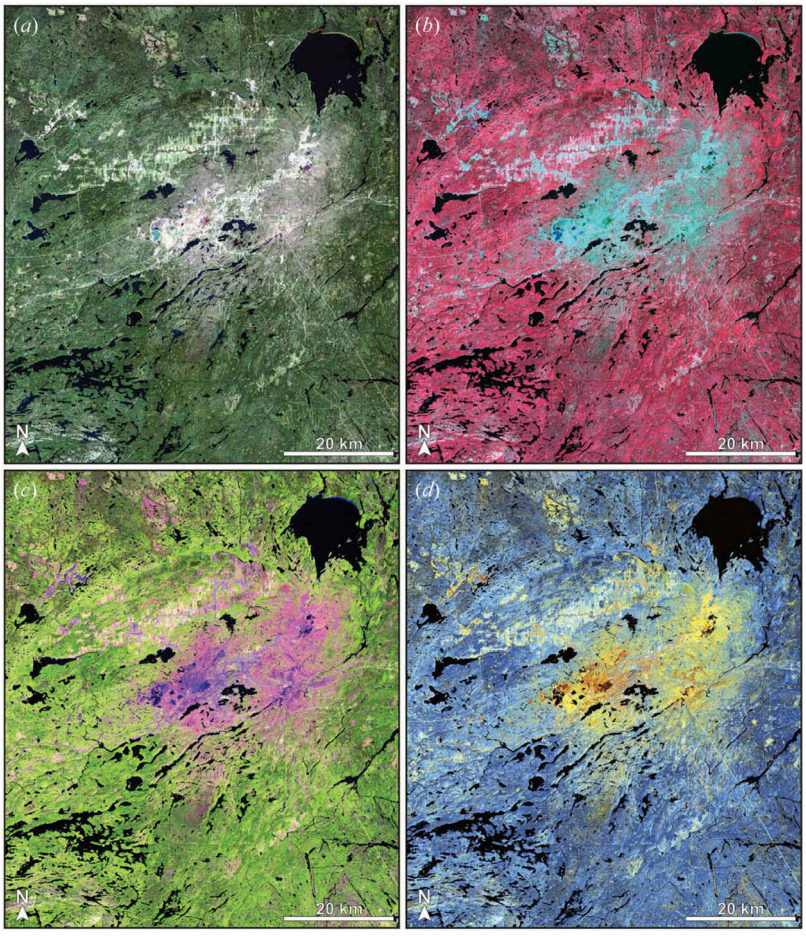

Figure 8. Colour composites of Landsat ETM+ reflectance data for the Sudbury study area: (*a*) 321-RGB (true colour); (*b*) 432-RGB (colour infrared); (*c*) 543-RGB; (*d*) 754-RGB. See Figure 1 for study area location.

Coated surfaces in the Sudbury study area were mapped in this study using the SAM algorithm, the Maximum Likelihood algorithm, and a neural network algorithm. The SAM classification method ranks the resemblance of the reflectance spectrum of a given endmember of interest to the reflectance properties of pixel locations in an image database (Kruse et al. 1993). This method treats reflectance spectra as vectors, and quantifies the resemblance between endmembers and pixel values on the basis of the angle between the spectra (e.g. van der Meer, Vazquez-Torres, and Van Dijk 1997; Williams et al. 2002; Rowan and Mars 2003; Qiu, Abdelsalam, and Thakkar 2006). A strength of the SAM algorithm is its potential utility in the identification of sites where a given class of interest is widely exposed, on the basis of the properties of a representative endmember reflectance spectrum of that class, without the need to identify and spectrally characterize all classes present in a study area (e.g. Othman and Gloaguen 2014). Techniques such as spectral mixture modelling, in contrast, generally require the spectral characterization of a comprehensive set of classes present in a study area, and typically produce poor results in geological mapping when used in conjunction with multispectral data sets such as those generated by Landsat sensors (e.g. van der Meer, Vazquez-Torres, and Van Dijk 1997; van der Meer and de Jong 2000; Leverington and Moon 2012). Surfaces on Earth are typically heterogeneous when sampled at pixel sizes of metres to tens of metres (e.g. Rogge et al. 2007), and thus a potential weakness of the SAM algorithm is that it highlights pixel locations associated with reflectance properties that are relatively close to those of endmembers, without explicitly taking into account the heterogeneity (and thus the associated spectral mixing) that typically exists at such pixel sizes (e.g. Galvão, Almeida-Filho, and Vitorello 2005). In this study, the Environment for Visualizing Images implementation of the SAM algorithm (Excelis 2014) was used to estimate the spatial distribution of coated bedrock surfaces in the Sudbury study area, using maximum spectral angles of 0.1, 0.2, 0.3, and 0.4 radians. The reflectance spectrum used to define black coatings in the SAM work was measured from a coated sample of the Copper Cliff Formation, which has reflectance properties that fall within the range typical of black coatings in the Sudbury region and is generally representative of black coatings here (Figure 6).

The Maximum Likelihood Classifier is among the most commonly used methods for the supervised classification of remote-sensing data (e.g. Ricchetti 2000; Nichol and Wong 2005; Richards 2012). This classifier is based on the assignment of conditional probabilities to each class involved in a classification, with class labels assigned to a given pixel location based on which class is associated with the highest probability for that pixel. Probability distributions are typically parameterized from vectors associated with training data on the basis of multivariate normal models. Thresholds can be optionally used to define a null class, in order to ensure that pixels are only labelled if the highest associated class probabilities exceed a preset minimum (e.g. Vinciková, Procházka, and Brom 2010). In the context of this study, a benefit of the Maximum Likelihood algorithm is that it does not rigidly define the reflectance characteristics of classes of interest, and in particular allows for the broader parameterization of class reflectance properties through the use of training sites that are characterized by both relatively pure and mixed spectra (e.g. both unvegetated and partly vegetated sites). A shortcoming of the Maximum Likelihood Classifier in the context of this study is its requirement that training data be collected for a comprehensive set of surface-cover classes for the study area of interest, rather than for the black coating class alone. In this study, the Geomatica implementation of the Maximum Likelihood algorithm (PCI 2014) was used to estimate the distribution of

coated bedrock surfaces. The following surface classes were defined: (1) deep water; (2) shallow or turbid water; (3) forest; (4) grassland; (5) clearing or urban; (6) coated bedrock; and (7) uncoated bedrock. The null-class option was enabled in order to allow pixel locations with reflectance properties outside those most characteristic of the above defined classes to be left as unclassified.

The feedforward backpropagation neural network algorithm is widely used in the classification of remote-sensing data (e.g. Benediktsson, Swain, and Ersoy 1990; An, Chung, and Rencz 1995; Leverington and Duguay 1997; Yang 1999; Leverington 2010; Leverington and Moon 2012; Cracknell and Reading 2014). This algorithm involves networks that consist of interconnected nodes whose weights and activations constrain how image values are related to surface classes. The values of network weights are iteratively determined during training through the process of backpropagation, in which the errors of output nodes are propagated backward through the network using the Delta Rule (Rumelhart and McClelland 1986; Gallant 1993). Once training is complete, weights become fixed and the network can be used in feedforward mode to classify new data sets, such that network flow proceeds strictly from input nodes towards output nodes. The parameterization of training data by neural networks is in some ways more widely applicable than that of the Maximum Likelihood Classifier, which assumes unimodal Gaussian distributions (Richards 2012). In this study, the Geomatica implementation of the neural network algorithm (PCI 2014) was used to estimate the distribution of coated bedrock surfaces. Surface classes were defined as described above for the Maximum Likelihood Classifier, and network properties were set based on standard principles (e.g. Gallant 1993; Bishop 1995; Reed and Marks 1999). Network geometry was defined with six nodes in the input layer (corresponding to the six ETM+ bands used as inputs), seven nodes in each of two intermediate layers, and seven nodes in the output layer (corresponding to the seven surface cover classes). Momentum and learning rate parameters were set to 0.9 and 0.1, respectively. Network weights were randomly initialized in the range of −0.5 to +0.5.

Outputs generated by the three algorithms were evaluated qualitatively on the basis of consistency with field experience in the study area. Outputs were evaluated quantitatively with regard to errors of omission through comparison of predicted coated sites with 1782 test pixels associated with 20 separate sites known to be predominantly characterized by coated bedrock. Outputs were evaluated with regard to errors of commission through comparison of predicted coated sites with 955 test pixels associated with known fully vegetated sites, 267 test pixels associated with known uncoated bedrock sites, 796 test pixels associated with known uncoated urban sites, and 2120 test pixels associated with known uncoated sites at clearings and open pits.

7. Classification results

The SAM, Maximum Likelihood, and neural network classification results are given for the Sudbury study area in Figures 9–11, respectively. SAM data are depicted for a maximum spectral angle of 0.3 radians, which generated optimum results. These results predict black coating distributions that are concentrated in the vicinities of the three main sites of past smelting activities in the Sudbury region. However, sites of coated bedrock are incorrectly discounted where partial vegetative cover is present. Furthermore, SAM results improperly label many uncoated urban sites (e.g. rooftops, paved roads, and airport runways) and uncoated clearings (e.g. unvegetated fields, and pits associated with mine tailings or aggregate mining activities) as being mantled by black coatings (Figure 9). The

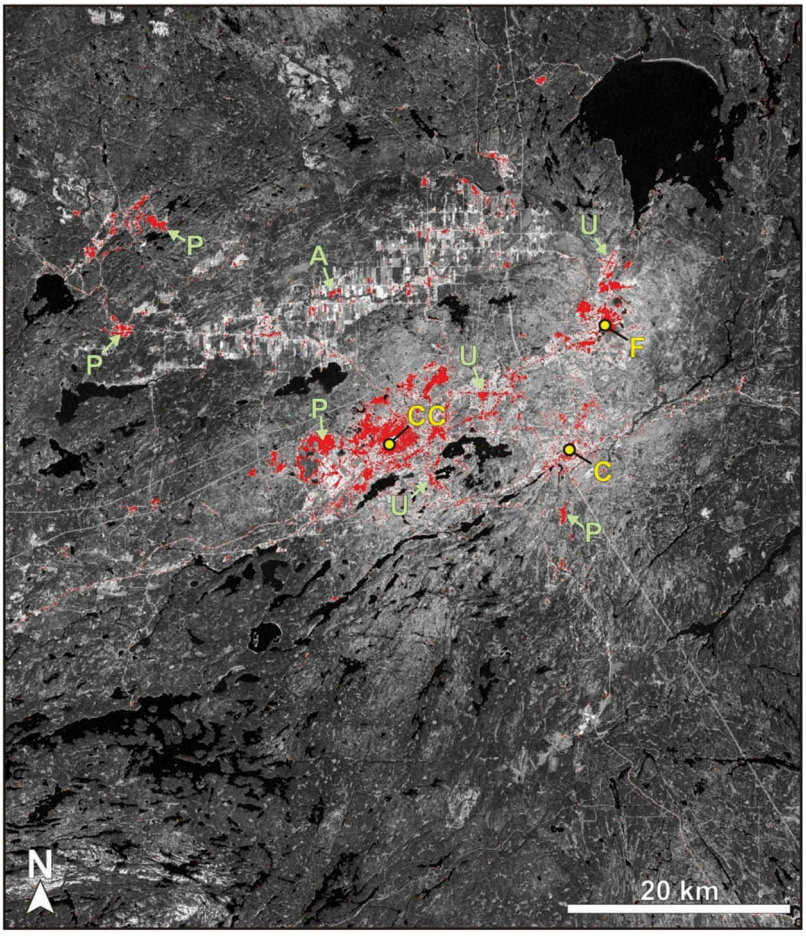

Figure 9. SAM-generated map of exposed rock surfaces in the study area that are mantled by black coatings (red), overlain on ETM+ band 3 reflectance data. This map is of limited utility since it discounts sites of coated bedrock where partial vegetative cover is present, and it erroneously identifies many uncoated urban (e.g. at 'U'), agricultural (e.g. at 'A'), and open-pit (e.g. at 'P') sites as coated. Mislabelled urban sites include rooftops, asphalt roads, and runway tarmac. Mislabelled open-pit sites include mine-tailings sites and areas of aggregate mining. Labelled smelter sites: F, Falconbridge; C, Coniston; CC, Copper Cliff. See Figure 1 for study area location.

generated database properly labels only 366 of the 1782 test pixels (20.5%) associated with known coated bedrock sites. None of the 955 test pixels representing known fully vegetated test sites, and none of the 267 test pixels representing known uncoated bedrock sites, were mislabelled as coated bedrock by the SAM algorithm. However, 460 of 796 test pixels (57.8%) representing known uncoated urban sites, and 1618 of 2120 test pixels (76.3%) representing known uncoated open pits and clearings, were mislabelled as coated bedrock. Thus, although the SAM database has a superficial resemblance to the distribution that might be expected of black coatings in the study area, it does not successfully discriminate between coated and non-coated sites, and is not a useful representation of the spatial distribution of bedrock mantled by black coatings.

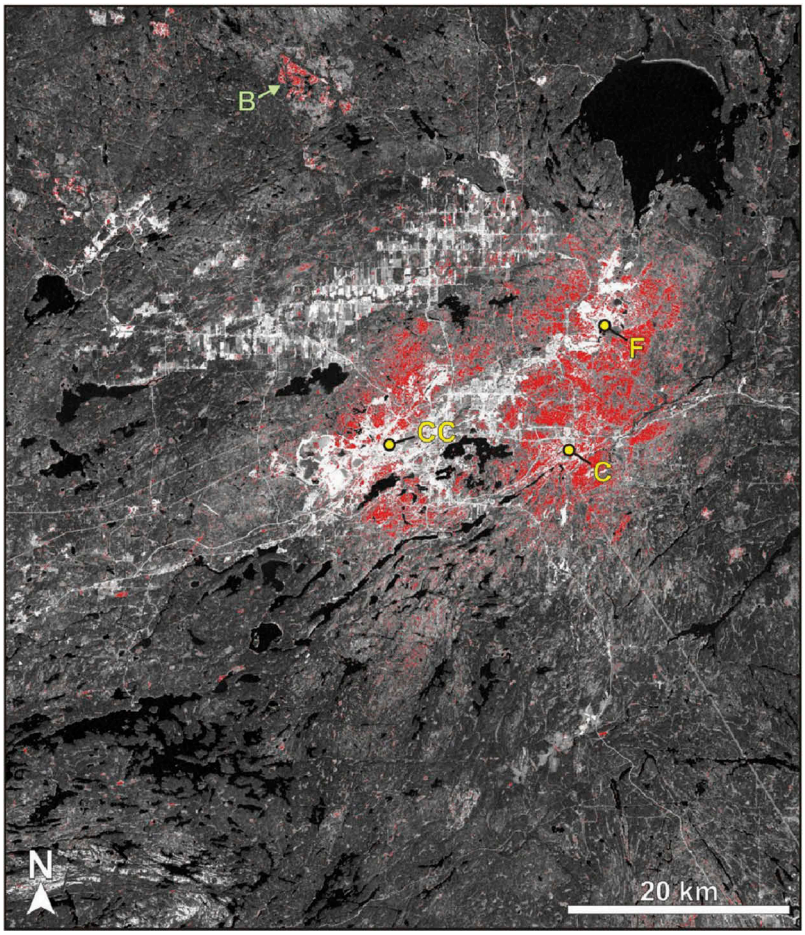

Figure 10. Maximum-Likelihood-generated map of exposed rock surfaces in the study area that are mantled by black coatings (red), overlain on ETM+ band 3 reflectance data. Although parts of exposed bedrock sites (e.g. at 'B') are incorrectly labelled as coated, this map otherwise correctly identifies the general locations of coated bedrock sites in the Sudbury region, and properly distinguishes these sites from uncoated urban features, aggregate pits, and other uncoated sites (compare with SAM results given in Figure 9). As expected, black coatings are most concentrated in areas that were previously characterized by moderate to heavy atmospheric sulphate and SO_2 concentrations (e.g. Figure 2). Labelled smelter sites: F, Falconbridge; C, Coniston; CC, Copper Cliff. See Figure 1 for study area location.

The Maximum Likelihood results (given for the coated class in Figure 10) similarly predict black coating distributions that fall mainly in the vicinities of the sites of past smelting in the Sudbury region. However, these distributions are more broadly dispersed across the study area, and much more closely reflect the true distribution of black coatings in the study area. Importantly, the uncoated urban or open pit sites that are problematic in the SAM-generated database are generally not mislabelled as sites mantled by black coatings in the Maximum Likelihood database, though parts of several patches of exposed bedrock in the northern part of the study area are mislabelled as coated by the classifier (Figure 10); bedrock exposed here consists of granitoids of the Superior Province (e.g.

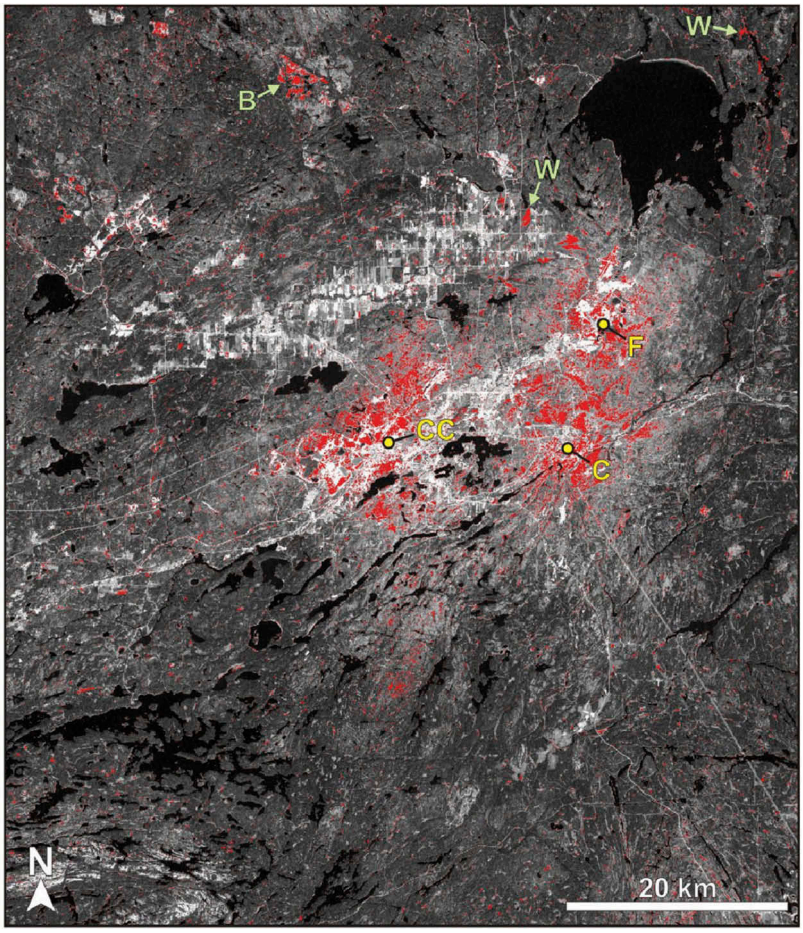

Figure 11. Neural-network-generated map of exposed rock surfaces in the study area that are mantled by black coatings (red), overlain on ETM+ band 3 reflectance data. As with the Maximum Likelihood results (Figure 10), parts of some exposed bedrock sites (e.g. at 'B') are incorrectly labelled as coated. Additionally, the presence of coated bedrock is erroneously predicted at some wetland sites such as fens and bogs (e.g. at 'W'). Although the neural network database is similar in character to the Maximum Likelihood database, it is characterized to a greater degree by errors of commission. Labelled smelter sites: F, Falconbridge; C, Coniston; CC, Copper Cliff. See Figure 1 for study area location.

Dressler 1984). The Maximum Likelihood database labels as coated 1208 of the 1782 test pixels (67.8%) associated with known coated bedrock sites. None of the 955 test pixels representing known fully vegetated sites was, and only 2 of 267 test pixels (0.7%) representing known uncoated bedrock sites were, mislabelled as coated bedrock by the Maximum Likelihood algorithm. Also, none of the 796 test pixels representing known uncoated urban sites was, and only 3 of 2120 test pixels (0.1%) representing known uncoated open pits and clearings were, mislabelled as coated bedrock. The use of the null class was a factor in reducing the percentage of coated sites successfully labelled, but its use helped to virtually eliminate the mislabelling of urban and open pit sites as coated, and did not negatively impact the overall validity of the predicted spatial distribution of coated

sites. Despite the limitations of the Maximum Likelihood database, it is a generally representative depiction of exposures of coated bedrock in the study area, properly highlighting areas extensively covered by coatings (located relatively close to past centres of smelting activities) as well as areas only discontinuously associated with coatings (e.g. at the granitoids of the Chief Lake Batholith, located in the southern part of the study area; Figure 1). As expected, the predicted spatial distribution of exposed black coatings is most concentrated in areas that were previously characterized by moderate to heavy atmospheric sulphate and SO_2 concentrations (e.g. Figure 2).

The neural network results (given for the coated class in Figure 11) are similar to those of the Maximum Likelihood Classifier, though they are characterized by additional examples of erroneous labelling of coated bedrock at certain wetland sites. The neural network database labels as coated 1260 of the 1782 test pixels (70.7%) associated with known coated bedrock sites, a proportion that is slightly higher than the 67.8% success rate of the Maximum Likelihood algorithm. Also, none of the 955 test pixels representing known fully vegetated sites and 267 test pixels representing known uncoated bedrock sites was mislabelled as coated bedrock by the neural network. However, 12 of the 796 test pixels (1.5%) representing known uncoated urban sites, and 153 of 2120 test pixels (7.2%) representing known uncoated open pits and clearings, were mislabelled as coated bedrock. Thus, although the neural network database is much more effective in describing the spatial distribution of coated bedrock in the Sudbury study area than the SAM database, its utility is compromised by its greater association with errors of commission relative to the Maximum Likelihood database.

8. Discussion

Reflectance spectra of black coatings in the Sudbury study area are relatively flat and featureless, and are characterized by low reflectance values across the visible, near-infrared, and short-wave infrared. Reflectance properties of coatings are similar to those of magnetite, a spinel-group mineral that is a common product of combustion and is typically present in the nanometre-to-micrometre-sized spheres in Sudbury coatings. If the lowered albedo and subdued absorption features of coatings are caused at least in part by the presence of nanometre-scale iron-bearing particles, these spectral effects may in some respects be related to those involved in space weathering (Hapke 2001). The presence of carbon-rich soot particles in the silica-rich parts of coatings may similarly be an important influence on the reflectance properties of coatings. Although K- and Fe-rich sulphate minerals are confirmed components of the Sudbury coatings, they do not introduce prominent absorption features in the reflectance spectra of coatings.

Black coatings effectively block the spectral features that would otherwise characterize the weathered surfaces of exposed bedrock in the study area. The capacity of black coatings to dominate the spectra of mantled geological materials is consistent with the known properties of coatings, including high densities of metal-rich particles and overall coating thicknesses of up to 200 μm. The absence of prominent peaks and troughs in the spectra of black coatings has the potential to make confident discrimination of these materials challenging.

Although the SAM-generated database of coated bedrock for the Sudbury study area highlights sites that are proximal to the three main smelter locations, it improperly associates numerous uncoated urban and unvegetated sites with the coated class (Figure 9). In contrast, the Maximum-Likelihood- and neural-network-generated databases more usefully distinguish between coated and uncoated sites. Overall, the Maximum Likelihood database (Figure 10) is the most useful depiction of the general spatial

distribution of exposed black coatings, in part because it is characterized by fewer errors of commission than the neural network database. The Maximum Likelihood results are not ideal, since only 67.8% of sites used here as test pixels for the coated class were successfully labelled as coated. However, this relatively low percentage is partly the result of the definition of a null class, which was very effective in preventing the widespread mislabelling of uncoated sites as coated without negatively impacting the overall validity of the produced map. Apart from issues noted above, the Maximum Likelihood database is qualitatively consistent with field experience in the study area.

The SAM algorithm produces optimum results in regions where the surface cover of pixels is simple and uniform rather than mixed (e.g. Galvão, Almeida-Filho, and Vitorello 2005), and the success of the Maximum Likelihood and neural network classifiers over the SAM classifier in this study is likely to be partly related to the capacity of these two algorithms for integration of partly vegetated but otherwise coated bedrock sites into the spectral definition of the coated class (through parameterization of the coated class signature using image-derived values). Successful utilization of the SAM algorithm is expected to have been further hindered by the relatively flat and indistinctive character of the reflectance spectra of black coatings in the Sudbury area. This algorithm only considers overall vector direction rather than vector length (e.g. Keshava and Mustard 2002; Qiu, Abdelsalam, and Thakkar 2006), and thus the many surface classes that have approximately flat reflectance characteristics (e.g. some forms of asphalt; Mei et al. 2014) can, even when differences in overall albedo are substantial, be readily confused with an endmember of interest that is itself characterized by flat reflectance. The SAM algorithm is not well suited to applications in which the most important factor in distinguishing between classes is albedo rather than spectrum shape (Murphy, Monteiro, and Schneider 2012). SAM results may have also been undermined by the relatively low spectral resolution of the utilized Landsat database, which is coarse relative to the resolution of the available endmember spectrum for the coated class. The SAM technique can be especially effective when applied to hyperspectral data sets (e.g. Crósta, Sabine, and Taranik 1998; Alberotanza 1999; Debba et al. 2005; Bauriegel et al. 2011), and in future research will be tested in its utility for the detection of black coatings in the Sudbury area using hyperspectral images.

Local contamination of soils in the Sudbury region is expected to slowly decrease as a result of smelter improvements and closures in recent decades, though substantial improvements in this regard are likely to take centuries (Meadows and Watmough 2012). Black coatings are eventually lost through processes including leaching and physical weathering, and therefore the mapping of black coatings in the Sudbury region is likely to be most useful in the monitoring of the gradual degradation of these coatings. At present, the mapping of black coatings is facilitated in the Sudbury region by the typical lack of continuous vegetation across bedrock sites that are widely mantled by these coatings, and sites at which future vegetation regrowth significantly outpaces the degradation of black coatings are less likely to be detected in future remote-sensing-based surveys of black coatings. Remote-sensing techniques such as those investigated in this study have the potential to be used in the discrimination and monitoring of ongoing environmental degradation in the vicinities of smelting activities in other locations around the world. Where the negative effects of smelting have been moderated or eliminated, these techniques may be useful in the monitoring of environmental recovery.

9. Conclusions

Black bedrock coatings remain a prominent vestige of past environmental degradation in the Sudbury region. The reflectance spectra of black coatings here are relatively flat and featureless, and are characterized by reflectance values of under ~13% across the visible, near-infrared, and short-wave infrared. Reflectance properties are similar to those of magnetite, a spinel-group mineral known to be a typical component of Sudbury coatings. The presence of carbon-rich soot particles in the Si-gel matrix of coatings may be an important influence on the reflectance properties of coatings. Black coatings can effectively block the spectral features of underlying bedrock, regardless of substrate lithology.

SAM-derived classification results predict black coating distributions that are concentrated in the vicinities of the three main sites of past smelting activities in the Sudbury region, but improperly label many uncoated urban sites and uncoated clearings as mantled by black coatings. In contrast, results generated by the Maximum Likelihood and neural network classifiers properly depict the more extensive distribution of black coatings in the study area, without most of the mislabelling that characterizes the SAM results. Results generated by the Maximum Likelihood Classifier are superior to those of the neural network, with the latter characterized to a greater degree by errors of commission. The mapping of black coatings using remote-sensing methods can provide information regarding the spatial character of environmental degradation in the vicinity of smelters, and should be helpful in the monitoring of environmental recovery where emissions have been reduced or eliminated, or where reclamation efforts (liming of soils and reforestation) have reduced the areal extent of barren land.

Acknowledgements

We thank Bill Morris, Timothy Warner, and an anonymous reviewer for their helpful comments. Michael Schindler and Kelly Malcolm were supported by a grant from the Natural Sciences and Engineering Research Council of Canada.

Disclosure statement

No potential conflict of interest was reported by the authors.

References

Abercrombie, J. M., M. Stewart, M. R. Rao, and M. E. Essington. 2011. "Aluminium Accumulation in *Pteris Cretica* and Trace Element Uptake in Vegetation Growing on an Abandoned Aluminium Smelter Site in Knoxville, TN, USA." *International Journal of Environment and Pollution* 45: 310–326.

Abuelgasim, A., C.-J. Chung, C. Champagne, K. Staenz, S. Monet, and K. Fung. 2005. Use of Multi-Temporal Remotely Sensed Data for Monitoring Land Reclamation in Sudbury, Ontario (Canada). *International Workshop on the Analysis of Multi-Temporal Remote Sensing Images*, 16–18 May, Institute of Electrical and Electronics Engineers, pp. 229–235. doi:10.1109/AMTRSI.2005.1469879.

Alberotanza, L. 1999. "Hyperspectral Aerial Images. A Valuable Tool for Submerged Vegetation Recognition in the Orbetello Lagoons, Italy." *International Journal of Remote Sensing* 20: 523–533. doi:10.1080/014311699213316.

Allum, J. A. E., and B. R. Dreisinger. 1987. "Remote Sensing of Vegetation Change Near Inco's Sudbury Mining Complexes." *International Journal of Remote Sensing* 8: 399–416. doi:10.1080/01431168708948649.

Alpay, S., J. J. Veillette, A. S. Dixit, and S. S. Dixit. 2006. "Regional and Historical Distributions of Lake-Water pH within a 100-Km Radius of the Horne Smelter in Rouyn-Noranda, Quebec, Canada." *Geochemistry: Exploration, Environment, Analysis* 6: 179–186.

An, P., C. F. Chung, and A. N. Rencz. 1995. "Digital Lithology Mapping from Airborne Geophysical and Remote Sensing Data in the Melville Peninsula, Northern Canada, Using a Neural Network Approach." *Remote Sensing of Environment* 53: 76–84. doi:10.1016/0034-4257(95)00041-X.

Bagatto, G., and M. A. Alikhan. 1987. "Zinc, Iron, Manganese, and Magnesium Accumulation in Crayfish Populations near Copper-Nickel Smelters at Sudbury, Ontario, Canada." *Bulletin of Environmental Contamination and Toxicology* 38: 1076–1081. doi:10.1007/BF01609098.

Bagatto, G., and J. D. Shorthouse. 1996. "Accumulation of Cu and Ni in Successive Stages of *Lymantria Dispar* L. (Lymantriidae, Lepidoptera) Near Ore Smelters at Sudbury, Ontario, Canada." *Environmental Pollution* 92: 7–12. doi:10.1016/0269-7491(95)00092-5.

Barcan, V., and E. Kovnatsky. 1998. "Soil Surface Geochemical Anomaly around the Copper-Nickel Metallurgical Smelter." *Water, Air, and Soil Pollution* 103: 197–218. doi:10.1023/A:1004930316648.

Barnett, P. J., and A. F. Bajc. 2002. "Quaternary Geology." In *The Physical Environment of the City of Greater Sudbury*, edited by D. H. Rousell and K. J. Jansons, Special Volume 6, 57–85, Sudbury: Ontario Geological Survey.

Bauriegel, E., A. Giebel, M. Geyer, U. Schmidt, and W. B. Herppich. 2011. "Early Detection of *Fusarium* Infection in Wheat Using Hyper-Spectral Imaging." *Computers and Electronics in Agriculture* 75: 304–312. doi:10.1016/j.compag.2010.12.006.

Behnia, P., J. R. Harris, R. H. Rainbird, M. C. Williamson, and M. Sheshpari. 2012. "Remote Predictive Mapping of Bedrock Geology Using Image Classification of Landsat and SPOT Data, Western Minto Inlier, Victoria Island, Northwest Territories, Canada." *International Journal of Remote Sensing* 33: 6876–6903. doi:10.1080/01431161.2012.693219.

Benediktsson, J. A., P. H. Swain, and O. K. Ersoy. 1990. "Neural Network Approaches versus Statistical Methods in Classification of Multisource Remote Sensing Data." *IEEE Transactions on Geoscience and Remote Sensing* 28: 540–552. doi:10.1109/TGRS.1990.572944.

Bishop, C. M. 1995. *Neural Networks for Pattern Recognition*. New York: Oxford University Press.

Bishop, J. L., and E. Murad. 2005. "The Visible and Infrared Spectral Properties of Jarosite and Alunite." *American Mineralogist* 90: 1100–1107. doi:10.2138/am.2005.1700.

Buzek, F., and J. Šrámek. 1985. "Sulfur Isotopes in the Study of Stone Monument Conservation." *Studies in Conservation* 30: 171–176. doi:10.1179/sic.1985.30.4.171.

Card, K. D. 1978a. "Metamorphism of the Middle Precambrian (Alphebian) of the Eastern Southern Province." In *Metamorphism in the Canadian Shield*, edited by J. A. Fraser and W. W. Heywood, Paper 78-10, 269–282. Ottawa, ON: Geological Survey of Canada.

Card, K. D., 1978b, *Geology of the Sudbury-Manitoulin Area, Districts of Sudbury and Manitoulin*. Report 166, Ontario Geological Survey, Sudbury.

Champagne, C. M., A. Abuelgasim, K. Staenz, S. Monet, and H. P. White, 2004, "Ecological Restoration from Space: The Use of Remote Sensing for Monitoring Land Reclamation in Sudbury." Society for Ecological Restoration, 16th International Conference, Victoria, August 24–26.

Chemtob, S. M., B. L. Jolliff, G. R. Rossman, J. M. Eiler, and R. E. Arvidson. 2010. "Silica Coatings in the Ka'u Desert, Hawaii, A Mars Analog Terrain: A Micromorphological, Spectral, Chemical, and Isotopic Study." *Journal of Geophysical Research* 115: E04001. doi:10.1029/2009JE003473.

Clark, R. N., G. A. Swayze, R. Wise, E. Livo, T. Hoefen, R. Kokaly, and S. J. Sutley. 2007. *USGS Digital Spectral Library Splib06a*. Digital Data Series 231. Reston, VA: United States Geological Survey.

Cloutis, E. A. 2011. "Spectral Reflectance Properties of Carbonaceous Chondrites: 1. CI Chondrites." *Icarus* 212: 180–209. doi:10.1016/j.icarus.2010.12.009.

Cloutis, E. A., M. J. Gaffey, and T. F. Moslow. 1994. "Spectral Reflectance Properties of Carbon-Bearing Materials." *Icarus* 107: 276–287. doi:10.1006/icar.1994.1023.

Cloutis, E. A., F. C. Hawthorne, S. A. Mertzman, K. Krenn, M. A. Craig, D. Marcino, M. Methot, J. Strong, J. F. Mustard, D. L. Blaney, J. F. Bell III, and F. Vilas. 2006. "Detection and Discrimination of Sulfate Minerals Using Reflectance Spectroscopy." *Icarus* 184: 121–157. doi:10.1016/j.icarus.2006.04.003.

Corfu, F., and A. Andrews. 1986. "A U-Pb Age for Mineralized Nipissing Diabase, Gowganda, Ontario." *Canadian Journal of Earth Sciences* 23: 107–109. doi:10.1139/e86-011.

Corfu, F., and R. M. Easton. 2001. "U-Pb Evidence for Polymetamorphic History of Huronian Rocks within the Grenville Front Tectonic Zone East of Sudbury, Ontario, Canada." *Chemical Geology* 172: 149–171. doi:10.1016/S0009-2541(00)00241-2.

Coulson, M. G., and E. M. Bridges. 1984. "The Remote Sensing of Contaminated Land." *International Journal of Remote Sensing* 5: 659–669. doi:10.1080/01431168408948849.

Cracknell, M., and A. M. Reading. 2014. "Geological Mapping Using Remote Sensing Data: A Comparison of Five Machine Learning Algorithms, Their Response to Variations in the Spatial Distribution of Training Data and the Use of Explicit Spatial Information." *Computers & Geosciences* 63: 22–33. doi:10.1016/j.cageo.2013.10.008.

Crósta, A. P., C. Sabine, and J. V. Taranik. 1998. "Hydrothermal Alteration Mapping at Bodie, California, Using AVIRIS Hyperspectral Data." *Remote Sensing of Environment* 65: 309–319. doi:10.1016/S0034-4257(98)00040-6.

Cui, Y.-J., Y.-G. Zhu, R.-H. Zhai, D.-Y. Chen, Y.-Z. Huang, Y. Qiu, and J.-Z. Liang. 2004. "Transfer of Metals from Soil to Vegetables in an Area Near a Smelter in Nanning, China." *Environment International* 30: 785–791. doi:10.1016/j.envint.2004.01.003.

Davidson, A. 2001. "The Chief Lake Complex Revisited, and the Problem of Correlation across the Grenville Front South of Sudbury, Ontario." *Precambrian Research* 107: 5–29. doi:10.1016/S0301-9268(00)00152-2.

Davidson, J., and J. Gunn. 2012. "Effects of Land Cover Disturbance on Stream Invertebrate Diversity and Metal Concentrations in a Small Urban Industrial Watershed." *Human and Ecological Risk Assessment: An International Journal* 18: 1078–1095. doi:10.1080/10807039.2012.707935.

Davies, B. E. 1983. "Heavy Metal Contamination from Base Metal Mining and Smelting: Implications for Man and His Environment." In *Applied Environmental Geochemistry*, edited by I. Thornton, 425–462. New York, NY: Academic Press.

Debba, P., F. J. A. Van Ruitenbeek, F. D. van der Meer, E. J. M. Carranza, and A. Stein. 2005. "Optimal Field Sampling for Targeting Minerals Using Hyperspectral Data." *Remote Sensing of Environment* 99: 373–386. doi:10.1016/j.rse.2005.05.005.

Dill, H. G. 2010. "The "Chessboard" Classification Scheme of Mineral Deposits: Mineralogy and Geology from Aluminum to Zirconium." *Earth-Science Reviews* 100: 1–420. doi:10.1016/j.earscirev.2009.10.011.

Dixon, J. C., C. E. Thorn, R. G. Darmody, and S. W. Campbell. 2002. "Weathering Rinds and Rock Coatings from an Arctic Alpine Environment, Northern Scandinavia." *Geological Society of America Bulletin* 114: 226–238. doi:10.1130/0016-7606(2002)114<0226:WRARCF>2.0.CO;2.

Dorn, R. I. 1998. *Rock Coatings*. New York, NY: Elsevier.

Dorn, R. I. 2009. "The Rock Varnish Revolution: New Insights from Microlaminations and the Contributions of Tanzhuo Liu." *Geography Compass* 3: 1804–1823. doi:10.1111/geco.2009.3.issue-5.

Dreisinger, B. R., and P. C. McGovern. 1969. *Sulphur Dioxide Levels and Resultant Injury to Vegetation in the Sudbury Area during the 1968 Season*. Sudbury: Ontario Department of Mines.

Dressler, B. O. 1984. *Sudbury Geological Compilation*. Map 2491, Precambrian Geology Series, 1:50,000. Sudbury: Ontario Geological Survey.

Durocher, J. L., and M. Schindler. 2011. "Iron-Hydroxide, Iron-Sulfate and Hydrous-Silica Coatings in Acid-Mine Tailings Facilities: A Comparative Study of Their Trace-Element Composition." *Applied Geochemistry* 26: 1337–1352. doi:10.1016/j.apgeochem.2011.05.007.

Easton, R. M. 1991. "The Grenville Province and the Proterozoic History of Central and Southern Ontario." In *Geology of Ontario*, edited by P. C. Thurston, H. R. Williams, R. H. Sutcliffe, and G. M. Stott, Special Volume 4, Part 2, 715–904. Sudbury: Ontario Geological Survey.

Excelis, 2014. *ENVI*. Boulder, CO: Excelis Visual Information Solutions. Accessed December 4. http://www.exelisvis.com/ProductsServices/ENVIProducts/ENVI.aspx

Farr, T. G., and J. B. Adams. 1984. "Rock Coatings in Hawaii." *Geological Society of America Bulletin* 95: 1077–1083.

Feng, M., J. O. Sexton, C. Huang, J. G. Masek, E. F. Vermote, F. Gao, R. Narasimhan, S. Channan, R. E. Wolfe, and J. R. Townshend. 2013. "Global Surface Reflectance Products from Landsat:

Assessment Using Coincident MODIS Observations." *Remote Sensing of Environment* 134: 276–293. doi:10.1016/j.rse.2013.02.031.

Flynn, L. P., A. J. L. Harris, and R. Wright. 2001. "Improved Identification of Volcanic Features Using Landsat 7 ETM+." *Remote Sensing of Environment* 78: 180–193. doi:10.1016/S0034-4257(01)00258-9.

Gaffey, S. J. 1985. "Reflectance Spectroscopy in the Visible and Near-Infrared (0.35-2.55 Mm): Applications in Carbonate Petrology." *Geology* 13: 270–273.

Gallant, S. I. 1993. *Neural Network Learning and Expert Systems*. Cambridge, MA: MIT Press.

Galvão, L. S., R. Almeida-Filho, and Í. Vitorello. 2005. "Spectral Discrimination of Hydrothermally Altered Materials Using ASTER Short-Wave Infrared Bands: Evaluation in a Tropical Savannah Environment." *International Journal of Applied Earth Observation and Geoinformation* 7: 107–114. doi:10.1016/j.jag.2004.12.003.

Garcia-Vallès, M., M. Vendrell-Saz, W. E. Krumbein, and C. Urzì. 1997. "Coloured Mineral Coatings on Monument Surfaces as a Result of Biomineralization: The Case of the Tarragona Cathedral (Catalonia)." *Applied Geochemistry* 12: 255–266. doi:10.1016/S0883-2927(96)00057-1.

Grieve, R. A. F., D. Ames, J. V. Morgan, and N. Artemieva. 2010. "The Evolution of the Onaping Formation at the Sudbury Impact Structure." *Meteoritics & Planetary Science* 45: 759–782. doi:10.1111/maps.2010.45.issue-5.

Hagner, O., and O. Rigina. 1998. "Detection of Forest Decline in Monchegorsk Area." *Remote Sensing of Environment* 63: 11–23. doi:10.1016/S0034-4257(97)00113-2.

Haneberg, W. C., G. S. Austin, and L. A. Brandvold. 1993. "Soil Lead Distribution at an Abandoned Smelter Site in Socorro, New Mexico." *Environmental Geology* 21: 90–95. doi:10.1007/BF00775056.

Hapke, B. 2001. "Space Weathering from Mercury to the Asteroid Belt." *Journal of Geophysical Research* 106: 10039–10073.

Harris, J. R., H. X. Juan, R. Rainbird, and P. Behnia. 2014. "Remote Predictive Mapping 6. A Comparison of Different Remotely Sensed Data for Classifying Bedrock Types in Canada's Arctic: Application of the Robust Classification Method and Random Forests." *Geoscience Canada* 41: 557–584.

Heale, E. L. 1995. "Integrated Management and Progressive Rehabilitation of Industrial Lands." In *Restoration and Recovery of an Industrial Region*, edited by J. M. Gunn, Springer Series on Environmental Management, 287–298. New York, NY: Springer-Verlag.

Heath, A. J., and P. F. Karrow. 2007. "Northernmost (?) Glacial Lake Algonquin Series Shorelines, Sudbury Basin, Ontario." *Journal of Great Lakes Research* 33: 264–278. doi:10.3394/0380-1330(2007)33[264:NGLASS]2.0.CO;2.

Hellmann, R., J.-M. Penisson, R. L. Hervig, J.-H. Thomassin, and M.-F. Abrioux. 2003. "An EFTEM/HRTEM High-Resolution Study of the near Surface of Labradorite Feldspar Altered at Acid pH: Evidence for Interfacial Dissolution Reprecipitation." *Physics and Chemistry of Minerals* 30: 192–197. doi:10.1007/s00269-003-0308-4.

Hutchinson, T. C., and L. M. Whitby. 1977. "The Effects of Acid Rainfall and Heavy Metal Particulates on a Boreal Forest Ecosystem near the Sudbury Smelting Region of Canada." *Water, Air, and Soil Pollution* 7: 421–438. doi:10.1007/BF00285542.

Jackson, S. L., and J. A. Fyon. 1991. "The Western Abitibi Subprovince in Ontario." In *Geology of Ontario*, edited by P. C. Thurston, H. R. Williams, R. H. Sutcliffe, and G. M. Stott, Special Volume 4, pt. 1, 405–482. Sudbury: Ontario Geological Survey.

Keays, R. R., and P. C. Lightfoot. 2004. "Formation of Ni-Cu-Platinum Group Element sulfide mineralization in the Sudbury Impact Melt Sheet." *Mineralogy and Petrology* 82: 217–258. doi:10.1007/s00710-004-0050-8.

Keller, W., J. H. Heneberry, and J. M. Gunn. 1999. "Effects of Emission Reductions from the Sudbury Smelters on the Recovery of Acid- and Metal-Damaged Lakes." *Journal of Aquatic Ecosystem Stress and Recovery* 6: 189–198. doi:10.1023/A:1009975116685.

Keshava, N., and J. F. Mustard. 2002. "Spectral Unmixing." *IEEE Signal Processing Magazine* 19: 44–57. doi:10.1109/79.974727.

Krinsley, D., J. Ditto, K. Langworthy, R. I. Dorn, and T. Thompson. 2013. "Varnish Microlaminations: New Insights from Focused Ion Beam Preparation." *Physical Geography* 34: 159–173.

Kruse, F. A., A. B. Lefkoff, J. W. Boardman, K. B. Heidebrecht, A. T. Shapiro, P. J. Barloon, and A. F. H. Goetz. 1993. "The Spectral Image Processing System (SIPS) – Interactive Visualization and Analysis of Imaging Spectrometer Data." *Remote Sensing of Environment* 44: 145–163. doi:10.1016/0034-4257(93)90013-N.

Lanteigne, S., M. Schindler, and A. M. McDonald. 2014. "Distribution of Metals and Metalloids in Smelter-Derived Particulate Matter in Soils and Mineralogical Insights into Their Retention and Release in a Low-T Environment." *The Canadian Mineralogist* 52: 453–471. doi:10.3749/canmin.52.3.453.

Lanteigne, S., M. Schindler, A. M. McDonald, K. Skeries, Y. Abdu, N. M. Mantha, M. Murayama, F. C. Hawthorne, and M. F. Hochella Jr. 2012. "Mineralogy and Weathering of Smelter-Derived Spherical Particles in Soils: Implications for the Mobility of Ni and Cu in the Surficial Environment." *Water, Air, & Soil Pollution* 223: 3619–3641. doi:10.1007/s11270-012-1135-3.

Le Deit, L., S. Le Mouélic, O. Bourgeois, J.-P. Combe, D. Mège, C. Sotin, A. Gendrin, E. Hauber, N. Mangold, and J.-P. Bibring. 2008. "Ferric Oxides in East Candor Chasma, Valles Marineris (Mars) Inferred from Analysis of Omega/Mars Express Data: Identification and Geological Interpretation." *Journal of Geophysical Research* 113: E07001. doi:10.1029/2007JE002950.

Leverington, D. W. 2010. "Discrimination of Sedimentary Lithologies Using Hyperion and Landsat Thematic Mapper Data: A Case Study at Melville Island, Canadian High Arctic." *International Journal of Remote Sensing* 31: 233–260. doi:10.1080/01431160902882637.

Leverington, D. W., and C. R. Duguay. 1997. "A Neural Network Method to Determine the Presence or Absence of Permafrost near Mayo, Yukon Territory, Canada." *Permafrost and Periglacial Processes* 8: 205–215. doi:10.1002/(ISSN)1099-1530.

Leverington, D. W., and W. M. Moon. 2012. "Landsat-TM-Based Discrimination of Lithological Units Associated with the Purtuniq Ophiolite, Quebec, Canada." *Remote Sensing* 4: 1208–1231. doi:10.3390/rs4051208.

Lévesque, J., and K. Staenz. 2008. "Monitoring Mine Tailings Revegetation Using Multitemporal Hyperspectral Image Data." *Canadian Journal of Remote Sensing* 34: S172–S186. doi:10.5589/m07-068.

Liu, T., and W. S. Broecker. 2007. "Holocene Rock Varnish Microstratigraphy and Its Chronometric Application in the Drylands of Western USA." *Geomorphology* 84: 1–21. doi:10.1016/j.geomorph.2006.06.008.

Loendorf, L. L. 1991. "Cation-Ratio Varnish Dating and Petroglyph Chronology in Southeastern Colorado." *Antiquity* 65: 246–255.

Mantha, N. M., M. Schindler, and T. K. Kyser. 2012. "Silica- and Sulfate-Bearing Rock Coatings in Smelter Areas: Part II. Forensic Tools for Atmospheric Metal(Loid)- and Sulfur-Isotope Compositions." *Geochimica et Cosmochimica Acta* 90: 221–241. doi:10.1016/j.gca.2012.05.013.

Mantha, N. M., M. Schindler, M. Murayama, and M. F. Hochella Jr. 2012. "Silica- and Sulfate-Bearing Rock Coatings in Smelter Areas: Products of Chemical Weathering and Atmospheric Pollution I. Formation and Mineralogical Composition." *Geochimica et Cosmochimica Acta* 85: 254–274. doi:10.1016/j.gca.2012.01.033.

Marcucci, E. C., B. M. Hynek, K. Kierein-Young, and K. L. Rogers. 2013. "Visible-Near-Infrared Reflectance Spectroscopy of Volcanic Acid-Sulfate Alteration in Nicaragua: Analogs for Early Mars." *Journal of Geophysical Research* 118: 2213–2233.

Masek, J. G., E. F. Vermote, N. E. Saleous, R. Wolfe, F. G. Hall, K. F. Huemmrich, F. Gao, J. Kutler, and T.-K. Lim. 2006. "A Landsat Surface Reflectance Dataset for North America, 1990–2000." *IEEE Geoscience and Remote Sensing Letters* 3: 68–72. doi:10.1109/LGRS.2005.857030.

Mayer, B., S. Alpay, W. D. Gould, L. Lortie, and F. Rosa. 2007. "The Onset of Anthropogenic Activity Recorded in Lake Sediments in the Vicinity of the Horne Smelter in Quebec, Canada: Sulfur Isotope Evidence." *Applied Geochemistry* 22: 397–414. doi:10.1016/j.apgeochem.2006.10.001.

McCall, J., J. Gunn, and H. Struik. 1995. "Photo Interpretive Study of Recovery of Damaged Lands Near the Metal Smelters of Sudbury, Canada." *Water, Air, & Soil Pollution* 85: 847–852. doi:10.1007/BF00476935.

McMartin, I., P. J. Henderson, A. Plouffe, and R. D. Knight. 2002. "Comparison of Cu-Hg-Ni-Pb Concentrations in Soils Adjacent to Anthropogenic Point Sources: Examples from Four Canadian Sites." *Geochemistry: Exploration, Environment, Analysis* 2: 57–73.

McSween, H. Y. Jr., G. J. Taylor, and M. B. Wyatt. 2009. "Elemental Composition of the Martian Crust." *Science* 324: 736–739. doi:10.1126/science.1165871.

Meadows, M., and S. A. Watmough. 2012. "An Assessment of Long-Term Risks of Metals in Sudbury: A Critical Loads Approach." *Water, Air, & Soil Pollution* 223: 4343–4354. doi:10.1007/s11270-012-1199-0.

Mei, A., R. Salvatori, N. Fiore, A. Allegrini, and A. D'Andrea. 2014. "Integration of Field and Laboratory Spectral Data with Multi-Resolution Remote Sensed Imagery for Asphalt Surface Differentiation." *Remote Sensing* 6: 2765–2781. doi:10.3390/rs6042765.

Meyn, H. D., 1970, *Geology of Hutton and Parkin Townships*. Geological Report 80, Ontario Department of Mines, Sudbury.

Mikkola, K. 1996. "A Remote Sensing Analysis of Vegetation Damage around Metal Smelters in the Kola Peninsula, Russia." *International Journal of Remote Sensing* 17: 3675–3690. doi:10.1080/01431169608949177.

Murphy, R. J., S. T. Monteiro, and S. Schneider. 2012. "Evaluating Classification Techniques for Mapping Vertical Geology Using Field-Based Hyperspectral Sensors." *IEEE Transactions on Geoscience and Remote Sensing* 50: 3066–3080. doi:10.1109/TGRS.2011.2178419.

Mussakowski, R. S. 1983. "A Technique for Mapping Environmental Change Using Digital Landsat Data." *Advances in Space Research* 2: 103–107. doi:10.1016/0273-1177(82)90227-7.

Narendrula, R., K. K. Nkongolo, and P. Beckett. 2012. "Comparative Soil Metal Analyses in Sudbury (Ontario, Canada) and Lubumbashi (Katanga, Dr-Congo)." *Bulletin of Environmental Contamination and Toxicology* 88: 187–192. doi:10.1007/s00128-011-0485-7.

Nesbitt, H. W., and G. M. Young. 1982. "Early Proterozoic Climates and Plate Motions Inferred from Major Element Chemistry of Lutites." *Nature* 299: 715–717. doi:10.1038/299715a0.

Nichol, J., and M. S. Wong. 2005. "Satellite Remote Sensing for Detailed Landslide Inventories Using Change Detection and Image Fusion." *International Journal of Remote Sensing* 26: 1913–1926. doi:10.1080/01431160512331314047.

Nkongolo, K. K., G. Spiers, P. Beckett, R. Narendrula, G. Theriault, A. Tran, and K. N. Kalubi. 2013. "Long-Term Effects of Liming on Soil Chemistry in Stable and Eroded Upland Areas in a Mining Region." *Water, Air, & Soil Pollution* 224 (7): 1–14. doi:10.1007/s11270-013-1618-x.

Othman, A. A., and R. Gloaguen. 2014. "Improving Lithological Mapping by SVM Classification of Spectral and Morphological Features: The Discovery of a New Chromite Body in the Mawat Ophiolite Complex (Kurdistan, NE Iraq)." *Remote Sensing* 6: 6867–6896. doi:10.3390/rs6086867.

PCI. 2014. *Geomatica*. Richmond Hill: PCI Geomatics. Accessed December 4. http://www.pcigeomatics.com/software/geomatica/professional

Pitblado, J. R., and B. D. Amiro. 1982. "Landsat Mapping of the Industrially Disturbed Vegetation Communities of Sudbury, Canada." *Canadian Journal of Remote Sensing* 8: 17–28. doi:10.1080/07038992.1982.10855020.

Pitblado, J. R., and E. A. Gallie. 1995. "Remote Sensing and Geographic Information Systems: Technologies for Mapping and Monitoring Environmental Health." In *Restoration and Recovery of an Industrial Region*, edited by J. M. Gunn, Springer Series on Environmental Management, 299–311. New York, NY: Springer-Verlag.

Qiu, F., M. Abdelsalam, and P. Thakkar. 2006. "Spectral Analysis of ASTER Data Covering Part of the Neoproterozoic Allaqi-Heiani Suture, Southern Egypt." *Journal of African Earth Sciences* 44: 169–180. doi:10.1016/j.jafrearsci.2005.10.009.

Reed, R. D., and R. J. Marks II. 1999. *Neural Smithing*. Cambridge, MA: MIT Press.

Riaza, A., and A. Müller. 2010. "Hyperspectral Remote Sensing Monitoring of Pyrite Mine Wastes: A Record of Climate Variability (Pyrite Belt, Spain)." *Environmental Earth Sciences* 61: 575–594. doi:10.1007/s12665-009-0368-y.

Ricchetti, E. 2000. "Multispectral Satellite Image and Ancillary Data Integration for Geological Classification." *Photogrammetric Engineering & Remote Sensing* 66: 429–435.

Richards, J. A. 2012. *Remote Sensing Digital Image Analysis: An Introduction*. New York, NY: Springer.

Richter, N., K. Staenz, and H. Kaufmann. 2008. "Spectral Unmixing of Airborne Hyperspectral Data for Baseline Mapping of Mine Tailings Areas." *International Journal of Remote Sensing* 29: 3937–3956. doi:10.1080/01431160801891788.

Rieuwerts, J., and M. Farago. 1996. "Heavy Metal Pollution in the Vicinity of a Secondary Lead Smelter in the Czech Republic." *Applied Geochemistry* 11: 17–23. doi:10.1016/0883-2927(95)00050-X.

Rigina, O. 2003. "Detection of Boreal Forest Decline with High-Resolution Panchromatic Satellite Imagery." *International Journal of Remote Sensing* 24: 1895–1912. doi:10.1080/01431160210154894.

Rigina, O., A. Baklanov, O. Hagner, and H. Olsson. 1999. "Monitoring of Forest Damage in the Kola Peninsula, Northern Russia Due to Smelting Industry." *The Science of the Total Environment* 229: 147–163. doi:10.1016/S0048-9697(99)00078-9.

Riller, U. 2005. "Structural Characteristics of the Sudbury Impact Structure, Canada: Impact-Induced versus Orogenic Deformation – A Review." *Meteoritics & Planetary Science* 40: 1723–1740. doi:10.1111/maps.2005.40.issue-11.

Rivard, B., R. E. Arvidson, I. J. Duncan, M. Sultan, and B. El Kaliouby. 1992. "Varnish, Sediment, and Rock Controls on Spectral Reflectance of Outcrops in Arid Regions." *Geology* 20: 295–298.

Rogge, D., B. Rivard, K. Segl, B. Grant, and J. Feng. 2014. "Mapping of Ni-Cu-Pge Ore Hosting Ultramafic Rocks Using Airborne and Simulated Enmap Hyperspectral Imagery, Nunavik, Canada." *Remote Sensing of Environment* 152: 302–317. doi:10.1016/j.rse.2014.06.024.

Rogge, D. M., B. Rivard, J. Zhang, A. Sanchez, J. Harris, and J. Feng. 2007. "Integration of Spatial-Spectral Information for the Improved Extraction of Endmembers." *Remote Sensing of Environment* 110: 287–303. doi:10.1016/j.rse.2007.02.019.

Rousell, D. H., W. Meyer, and S. A. Prevec. 2002. Bedrock Geology and Mineral Deposits. In: *The Physical Environment of the City of Greater Sudbury*, edited by D. H. Rousell and K. J. Jansons, Special Volume 6, 21–55. Sudbury: Ontario Geological Survey.

Rowan, L. C., and J. C. Mars. 2003. "Lithologic Mapping in the Mountain Pass, California Area Using Advanced Spaceborne Thermal Emission and Reflection Radiometer (ASTER) Data." *Remote Sensing of Environment* 84: 350–366. doi:10.1016/S0034-4257(02)00127-X.

Rumelhart, D. E., and J. L. McClelland. and the PDP Research Group. 1986. *Parallel Distributed Processing: Explorations in the Microstructure of Cognition* Vols. 1 and 2. Cambridge, MA: MIT Press.

Saarinen, O. W., and W. A. Tanos. 2002. "The Physical Environment of the Sudbury Area and Its Influence on Urban Development." In *The Physical Environment of the City of Greater Sudbury*, edited by D. H. Rousell and K. J. Jansons, Special Volume 6, 3–18. Sudbury: Ontario Geological Survey.

Sánchez, J. S., C. A. S. Alves, J. R. V. Vidal Romaní, and D. F. Mosquera. 2009. "Origin of Gypsum-Rich Coatings on Historic Buildings." *Water, Air, and Soil Pollution* 204: 53–68. doi:10.1007/s11270-009-0025-9.

Sanjurjo-Sánchez, J., J. R. V. Romaní, and C. Alves. 2012. "Comparative Analysis of Coatings on Granitic Substrates from Urban and Natural Settings (NW Spain)." *Geomorphology* 138: 231–242. doi:10.1016/j.geomorph.2011.09.008.

Schaepman-Strub, G., M. E. Schaepman, T. H. Painter, S. Dangel, and J. V. Martonchik. 2006. "Reflectance Quantities in Optical Remote Sensing – Definitions and Case Studies." *Remote Sensing of Environment* 103: 27–42. doi:10.1016/j.rse.2006.03.002.

Schiffman, P., R. Zierenberg, N. Marks, J. L. Bishop, and M. D. Dyar. 2006. "Acid-Fog Deposition at Kilauea Volcano: A Possible Mechanism for the Formation of Siliceous-Sulfate Rock Coatings on Mars." *Geology* 34: 921–924.

Schindler, M., J. Durocher, Y. Abdu, and F. C. Hawthorne. 2009. "Hydrous Silica Coatings: Occurrence, Speciation of Metals, and Environmental Significance." *Environmental Science & Technology* 43: 8775–8780. doi:10.1021/es9018817.

Schindler, M., N. Mantha, K. T. Kyser, M. Murayama, and M. F. Hochella Jr. 2012. "Shining Light on Black Rock Coatings in Smelter-Impacted Areas." *Geoscience Canada* 39: 148–157.

Seelos, K. D., R. E. Arvidson, B. L. Jolliff, S. M. Chemtob, R. V. Morris, D. W. Ming, and G. A. Swayze. 2010. "Silica in a Mars Analog Environment: Ka'u Desert, Kilauea Volcano, Hawaii." *Journal of Geophysical Research* 115: E00D15. doi:10.1029/2009JE003347.

Shang, J., B. Morris, P. Howarth, J. Lévesque, K. Staenz, and B. Neville. 2009. "Mapping Mine Tailing Surface Mineralogy Using Hyperspectral Remote Sensing." *Canadian Journal of Remote Sensing* 35: S126–S141. doi:10.5589/m10-001.

Shang, J., K. Staenz, J. Lévesque, P. Howarth, B. Morris, and L. Lanteigne. 2002. "Mine Tailings Characterization Using PROBE Data (Preliminary Results)." In *Proceedings of the* 2002 *International Geoscience and Remote Sensing Symposium*, 2921–2923. Toronto, ON: IEEE.

Sims, P. K., K. D. Card, G. B. Morey, and Z. E. Peterman. 1980. "The Great Lakes Tectonic Zone – A Major Crustal Structure in Central North America." *Geological Society of America Bulletin* 91: 690–698.

Singhroy, V., and F. Kuhn, 1996, "Remote Sensing for Characterizing and Monitoring of Hazardous Waste Sites – Case Studies in Canada and Germany." International Archives of Photogrammetry and Remote Sensing, Vol. XXXI, Part B7, Vienna.

Sultan, M., R. Arvidson, N. C. Sturchio, and E. A. Guinness. 1987. "Lithologic Mapping in Arid Regions with Landsat Thematic Mapper Data: Meatiq Dome, Egypt." *Geological Society of America Bulletin* 99: 748–762.

Svendsen, M. L., E. Steinnes, and H. A. Blom. 2007. "Vertical and Horizontal Distributions of Zn, Cd, Pb, Cu, and Hg in Uncultivated Soil in the Vicinity of a Zinc Smelter at Odda, Norway." *Soil & Sediment Contamination* 16: 585–603. doi:10.1080/15320380701623644.

Tanentzap, F. M., and P. Ryser. 2015. "Decreased Resistance to Embolism in Red Maple (*Acer Rubrum* L.) Saplings within a Heavy Metal Contaminated Region." *Environmental and Experimental Botany* 109: 40–44. doi:10.1016/j.envexpbot.2014.07.019.

Tani, Y., N. Miyata, K. Iwahori, M. Soma, S.-I. Tokuda, H. Seyama, and B. K. G. Theng. 2003. "Biogeochemistry of Manganese Oxide Coatings on Pebble Surfaces in the Kikukawa River System, Shizuoka, Japan." *Applied Geochemistry* 18: 1541–1554. doi:10.1016/S0883-2927(03)00075-1.

Tømmervik, H., K. A. Høgda, and I. Solheim. 2003. "Monitoring Vegetation Changes in Pasvik (Norway) and Pechenga in Kola Penninsula (Russia) Using Multitemporal Landsat MSS/TM Data." *Remote Sensing of Environment* 85: 370–388. doi:10.1016/S0034-4257(03)00014-2.

Tømmervik, H., B. E. Johansen, and J. P. Pedersen. 1995. "Monitoring the Effects of Air Pollution on Terrestrial Ecosystems in Varanger (Norway) and Nikel-Pechenga (Russia) Using Remote Sensing." *The Science of the Total Environment* 160–161: 753–767. doi:10.1016/0048-9697(95)04409-T.

Toutoubalina, O. V., and W. G. Rees. 1999. "Remote Sensing of Industrial Impact on Arctic Vegetation around Noril'sk, Northern Siberia: Preliminary Results." *International Journal of Remote Sensing* 20: 2979–2990. doi:10.1080/014311699211561.

van der Meer, F. 2004. "Analysis of Spectral Absorption Features in Hyperspectral Imagery." *International Journal of Applied Earth Observation and Geoinformation* 5: 55–68. doi:10.1016/j.jag.2003.09.001.

van der Meer, F., and S. M. De Jong. 2000. "Improving the Results of Spectral Unmixing of Landsat Thematic Mapper Imagery by Enhancing the Orthogonality of End-Members." *International Journal of Remote Sensing* 21: 2781–2797. doi:10.1080/01431160050121249.

van der Meer, F., M. Vazquez-Torres, and P. M. Van Dijk. 1997. "Spectral Characterization of Ophiolite Lithologies in the Troodos Ophiolite Complex of Cyprus and Its Potential in Prospecting for Massive Sulphide Deposits." *International Journal of Remote Sensing* 18: 1245–1257. doi:10.1080/014311697218395.

Vaughan, R. G., W. M. Calvin, and J. V. Taranik. 2003. "SEBASS Hyperspectral Thermal Infrared Data: Surface Emissivity Measurement and Mineral Mapping." *Remote Sensing of Environment* 85: 48–63. doi:10.1016/S0034-4257(02)00186-4.

Vinciková, H., J. Procházka, and J. Brom. 2010. "Timely Identification of Agricultural Crops in the Temelín NPP Vicinity Using Satellite Data in the Event of Radiation Contamination." *Journal of Agrobiology* 27: 73–83. doi:10.2478/s10146-009-0014-z.

Williams, D. J., J. M. Bigham, C. A. Cravotta III, S. J. Traina, J. E. Anderson, and J. G. Lyon. 2002. "Assessing Mine Drainage pH from the Color and Spectral Reflectance of Chemical Precipitates." *Applied Geochemistry* 17: 1273–1286. doi:10.1016/S0883-2927(02)00019-7.

Winterhalder, K. 1995. "Early History of Human Activities in the Sudbury Area and Ecological Damage to the Landscape." In *Restoration and Recovery of an Industrial Region*, edited by J. M. Gunn, Springer Series on Environmental Management, 17–31. New York: Springer-Verlag.

Winterhalder, K. 2002. "The Effects of the Mining and Smelting Industry on Sudbury's Landscape." In *The Physical Environment of the City of Greater Sudbury*, edited by D. H. Rousell and K. J. Jansons, 145–173. Special Volume 6. Sudbury: Ontario Geological Survey.

Xiong, Y., S. D. Khan, K. Mahmood, and V. B. Sisson. 2011. "Lithological Mapping of Bela Ophiolite with Remote-Sensing Data." *International Journal of Remote Sensing* 32: 4641–4658. doi:10.1080/01431161.2010.489069.

Yang, H. 1999. "A Back-Propagation Neural Network for Mineralogical Mapping from AVIRIS Data." *International Journal of Remote Sensing* 20: 97–110. doi:10.1080/014311699213622.

Zajzon, N., E. Márton, P. Sipos, F. Kristály, T. Németh, V. Kis-Kovács, and T. G. Weiszburg. 2013. "Integrated Mineralogical and Magnetic Study of Magnetic Airborne Particles from Potential Pollution Sources in Industrial-Urban Environment." *Carpathian Journal of Earth and Environmental Sciences* 8: 179–186.

Zhang, J., B. Rivard, and A. Sanchez-Azofeifa. 2004. "Derivative Spectral Unmixing of Hyperspectral Data Applied to Mixtures of Lichen and Rock." *IEEE Transactions on Geoscience and Remote Sensing* 42: 1934–1940. doi:10.1109/TGRS.2004.832239.

Zubareva, O. N., L. N. Skripal'shchikova, N. V. Greshilova, and V. I. Kharuk. 2003. "Zoning of Landscapes Exposed to Technogenic Emissions from the Norilsk Mining and Smelting Works." *Russian Journal of Ecology* 34: 375–380. doi:10.1023/A:1027356316112.